SpaceMath v.2.0 with machine learning. A Mathematica package for beyond the standard model parameter space searches

M. A. Arroyo-Ureña

Facultad de Ciencias Físico-Matemáticas, Benemérita Universidad Autónoma de Puebla, 72570, Puebla, Pue., México.
Centro Interdisciplinario de Investigación y Enseñanza de la Ciencia, Benemérita Universidad Autónoma de Puebla, 72570, Puebla, Pue., México.
e-mail: marco.arroyo@fcfm.buap.mx

T. A. Valencia-Pérez

Instituto de Física, Universidad Nacional Autónoma de México, 01000, CDMX, México.
e-mail: tvalencia@fisica.unam.mx

Received 27 September 2024; accepted 21 February 2025

SpaceMath v.2.0 with Machine Learning is an extension of SpaceMath v.1.0 and implements processes with Flavor-Changing Neutral Currents at tree and one-loop level, namely, i) Radiative decays $\ell_i \to \ell_j\gamma$, ii) $\ell_i \to \ell_j\ell_k\bar{\ell}_k$ decays ($\ell_i = \tau,\ \mu$, $\ell_{j,\,k} = \mu,\ e$, with $\ell_i \neq \ell_j \neq \ell_k$), iii) anomalous magnetic moment of the muon δa_μ and iv) decays $B^0_{s,d} \to \mu^-\mu^+$. In addition to scanning parameter spaces, SpaceMath v.2.0 has a novel implementation that make use of Machine Learning algorithms to predict Benchmark Points for numerical evaluations of observables in particle physics. A detailed example applied to the *Two-Higgs Doublet Model of type III* parameter space is developed.

Keywords: 2HDM; Machine Learning.

DOI: https://doi.org/10.31349/RevMexFisE.23.020201

1. Introduction

Our current knowledge of elementary particles and their interactions is based on solid theoretical foundations that are embodied in the Standard Model (SM). This theory provides a description of the weak, strong and electromagnetic interactions, explaining almost all experimental observations, except for isolated cases. However, despite these achievements, there are phenomena that the SM cannot explain, for example: the hierarchy problem, the origin of dark matter, the problem of flavor, etc. The fact that the SM cannot provide an answer to these phenomena suggests physics Beyond the SM (BSM). In the last decades, several extensions of the SM have been presented to try to solve them [1–16]. The price to pay is the emergence of free parameters that are not predicted by the theory. From a phenomenological point of view, one frequently finds these free parameters which should be constrained in some way, but at same time motivated and allowed by experimental measurements or by theoretical restrictions. With the SpaceMath package, it is possible to do it. Free model parameter spaces can be constrained automatically within a friendly interface and an intuitive environment, where the user defines the couplings and executing the commands of SpaceMath to generate both plots and tables which show areas and numerical values, respectively, according to experimental data. Similar packages to SpaceMath can be consulted in the Refs. [17–23]. However, SpaceMath has the feature that it only requires the installation of Wolfram Mathematica (available in many universities and research institutes) and a very basic knowledge of Wolfram language. Unlike other programs that require prior knowledge of programming languages, the SpaceMath package has a fast learning curve and a practical approach which makes it an option for quick results.

The organization of our work is as follows. In Sec. 2 we present the theoretical framework necessary to have the basis of the programming of SpaceMath. Section. 3 shows a concise to install SpaceMath v.2.0 and how it works, giving a detailed example. Section 4 is focused on the validation of SpaceMath v.2.0 by reproducing several results shown in the literature. Finally, conclusion and perspectives are presented in Sec. 5.

2. A theoretical overview

We have implemented in SpaceMath v.2.0 LHC Higgs boson data (as well as projections for the HL-LHC and HE-LHC) and Lepton Flavor Violating processes (LFV). The former can be applied to any model that predicts corrections to the Higgs-fermions and Higgs-V ($V = W, Z$) couplings, while the LFV processes only can be studied for models with Flavor Changing Neutral Interactions at tree level. Specifically to models with both real and complex singlets, real and complex doublets and effective theories. We start describing the theoretical framework in which SpaceMath

`v.2.0` works. Namely:

1. Higgs boson data
   (a) Signal strength modifiers $\mathcal{R}_X$,
   (b) Higgs boson coupling modifiers κ_i.
2. LFV processes
   (a) $h \to \ell_i \ell_j$,
   (b) Radiative processes $\ell_i \to \ell_j \gamma$,
   (c) Muon anomalous magnetic moment a_μ,
   (d) $\ell_i \to \ell_j \ell_j \ell_k$ decays,
   (e) $B^0_{s,\,d} \to \mu^+ \mu^-$.

2.1. LHC Higgs boson data

2.1.1. Signal strength modifiers $\mathcal{R}_X$

For a production process $\sigma(pp \to H_i)$ and a decay $H_i \to X$, the signal strength is defined as follows:

$$\mathcal{R}_X = \frac{\sigma(pp \to h) \cdot \mathcal{BR}(h \to X)}{\sigma(pp \to h^{\rm SM}) \cdot \mathcal{BR}(h^{\rm SM} \to X)}, \qquad (1)$$

where $\sigma(pp \to H_i)$ is the production cross section of H_i, with $H_i = h,\, h^{\rm SM}$; here h is the SM-like Higgs boson coming from an extension of the SM and $h^{\rm SM}$ is the SM Higgs boson; $\mathcal{BR}(H_i \to X)$ is the branching ratio of the decay $H_i \to X$, with $X = b\bar{b}$, $\tau^-\tau^+$, WW^*,ZZ^*, $\gamma\gamma$.

2.1.2. Higgs boson coupling modifiers κ_i

The coupling modifiers κ_i are introduced to quantify the deviations of the SM-like Higgs boson to other particles. The coupling modifiers κ_i for a production cross section or a decay mode, are defined as follows:

$$\kappa^2_{pp} = \frac{\sigma(pp \to h)}{\sigma(pp \to h^{\rm SM})}, \quad \text{or} \quad \kappa^2_X = \frac{\Gamma(h \to X)}{\Gamma(h^{\rm SM} \to X)}. \qquad (2)$$

We consider tree-level Higgs boson couplings to different particles, *i.e.*, g_{hZZ^*}, g_{hWW^*}, $g_{h\tau^-\tau^+}$, $g_{h\mu^-\mu^+}$, $g_{hb\bar{b}}$, as well as effective coupling modifiers g_{hgg} and $g_{h\gamma\gamma}$ which describe gluon fusion production `ggh` and the $h \to \gamma\gamma$ decay, respectively.

TABLE I. Experimental measurements on the $\mathcal{R}_X$ implemented in `SpaceMath v2.0`

$\mathcal{R}_X$	Value [24]
$\mathcal{R}_{b\bar{b}}$	0.99 ± 0.12
$\mathcal{R}_{\tau^-\tau^+}$	0.91 ± 0.09
$\mathcal{R}_{WW^*}$	1.00 ± 0.08
$\mathcal{R}_{ZZ^*}$	1.02 ± 0.08
$\mathcal{R}_{\gamma\gamma}$	1.10 ± 0.06

TABLE II. Current bounds of the observables implemented in `SpaceMath v2.0`.

Observable	Bound [24]
$\mathcal{BR}(h \to e\mu)$	$< 4.4 \times 10^{-5}$
$\mathcal{BR}(h \to e\tau)$	$< 2 \times 10^{-3}$
$\mathcal{BR}(h \to \mu\tau)$	$< 1.5 \times 10^{-3}$
$\mathcal{BR}(\mu \to e\gamma)$	$< 4.2 \times 10^{-13}$
$\mathcal{BR}(\tau \to e\gamma)$	$< 3.3 \times 10^{-8}$
$\mathcal{BR}(\tau \to \mu\gamma)$	$< 4.2 \times 10^{-8}$
$\mathcal{BR}(\tau \to 3e)$	$< 2.7 \times 10^{-8}$
$\mathcal{BR}(\tau \to 3\mu)$	$< 2.1 \times 10^{-8}$
$\mathcal{BR}(\mu \to 3e)$	$< 1.0 \times 10^{-12}$

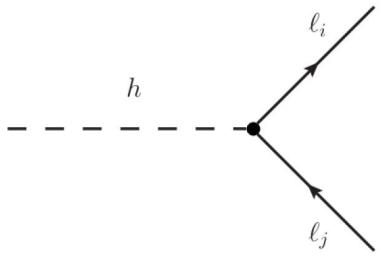

FIGURE 1. Feynman diagram of the decay $h \to \ell_i \ell_j$. This decay can constrain parameters involved in the $h\ell_i\ell_j$ interaction, as indicated by black circle.

2.2. Lepton Flavor Violating processes

Let us first to show in Table II all the upper limits that correspond to each individual process presented below.

2.2.1. $h \to \ell_i \ell_j$ decays

The LFV processes $h \to \ell_i \ell_j$ ($\ell_{i,\,j} = \ell^-_{i,\,j} \ell^+_{i,\,j}$) where $\ell_i \ell_j = e\mu,\, e\tau,\, \tau\mu$ can arise at tree level in many models that extend to the SM. The relevant interactions can be extrated from the Yukawa Lagrangian

$$\mathcal{L}_Y \supset -Y_{ij} \bar{\ell}^i_L \ell^j_R h + h.c. \qquad (3)$$

The correponding full decay width of the $h \to \ell_i \ell_j$ decays is given by:

$$\Gamma(h \to \bar{f}_i f_j) = \frac{N_c g^2_{h\bar{f}_i f_j} m_h}{128\pi} \left[4 - (\sqrt{\tau_{f_i}} + \sqrt{\tau_{f_j}})^2 \right]^{3/2} \times \sqrt{4 - (\sqrt{\tau_{f_i}} - \sqrt{\tau_{f_j}})^2}, \qquad (4)$$

where $g_{h\bar{f}_i f_j}$ is the $h\bar{f}_i f_j$ coupling coming from an extension of the SM, $Nc = 3\,(1)$ is the color number for quarks (leptons), m_h is the Higgs boson mass and $\tau_i = 4m_i^2/m_h^2$. Note that in general $i \neq j$ and f denotes a fermion, particularly $f_{i,j} = \ell_{i,j}$. Figure 1 presents the Feynman diagram at tree-level that contribute to the process $h \to \ell_i \ell_j$.

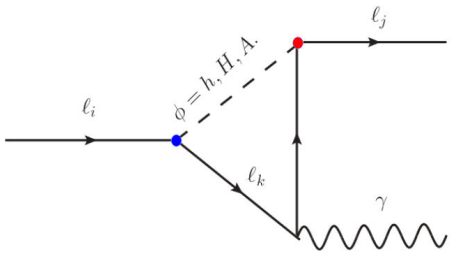

FIGURE 2. Feynman diagram that contribute to the decay $\ell_i \to \ell_j\gamma$. This process constrains parameters that are a function of the $\phi\ell_i\ell_k$ and $\phi\ell_k\bar{\ell}_j$ LFV interactions, blue and red circles, respectively.

2.2.2. *Decays $\ell_i \to \ell_j\gamma$*

The Feynman diagram that contribute to the process $\ell_i \to \ell_j\gamma$ is presented in Fig. 2.

The effective Lagrangian for the $\ell_i \to \ell_j\gamma^i$ is given by

$$\mathcal{L}_{\text{eff}} = C_L Q_{L\gamma} C_R Q_{R\gamma} + h.c., \tag{5}$$

where the dim-5 electromagnetic penguin operators read

$$Q_{L\gamma,\,R\gamma} = \frac{e}{8\pi^2}(\bar{\ell}_j\sigma^{\alpha\beta}P_{L,\,R}\ell_i)F_{\alpha\beta}, \tag{6}$$

here $F_{\alpha\beta}$ is the electromagnetic field strength tensor. The Wilson coefficients $C_{L,\,R}$ receive contributios at one-loop level and an important contribution from Barr-Zee two-loops level. For the particular case when $\ell_i = \tau$ and $\ell_j = \mu$, we assume the approximations $g_{\phi\mu\mu} \ll g_{\phi\tau\tau}$ and $m_\mu \ll m_\tau \ll m_\phi$. Under this assertion the one-loop Wilson coefficients $C_{L,\,R}$ simplify as follows [25, 26]

$$C_L^{\text{1loop}} \simeq \sum_\phi \frac{g_{\phi\tau\tau}g_{\phi\tau\mu}}{12m_\phi^2}\left(-4 + 3\log\frac{m_\phi^2}{m_\tau^2}\right),$$

$$C_R^{\text{2loop}} \simeq \sum_\phi \frac{g_{\phi\tau\tau}g_{\phi\tau\mu}}{12m_\phi^2}\left(-4 + 3\log\frac{m_\phi^2}{m_\tau^2}\right). \tag{7}$$

The numerical expressions for 2-loop contributions are given by

$$C_L^{\text{2loop}} = \sum_\phi g^*_{\phi\tau\mu}(-0.082 g_{\phi tt} + 0.11)/(m_\phi \text{GeV})^2. \tag{8}$$

The rate for $\tau \to \mu\gamma$ is

$$\Gamma(\tau \to \mu\gamma) = \frac{\alpha m_\tau^2}{64\pi^4}(|C_L|^2 + |C_R|^2). \tag{9}$$

To obtain the corresponding width decay of the processes $\mu \to e\gamma$ and $\tau \to e\gamma$, the replacements $\tau \to \mu$, $\mu \to e$ for the first decay and $\mu \to e$ for the second process from (5) to (9) are required.

2.2.3. *Muon anomalous magnetic moment (μAMM)*

The Feynman diagrams that contribute to μAMDM are shown in Fig. 3

The one-loop contribution for diagram in Fig. 3a) is given by

$$a_\mu = \frac{m_\mu}{16\pi^2}\sum_{\ell=e,\,\mu,\,\tau}\sum_{\phi=h,\,H,\,A}\frac{m_\ell g_{\phi\mu\ell}}{m_\phi^2} \times \left(2\ln\left(\frac{m_{\phi^2}}{m_\ell^2}\right) - 3\right), \tag{10}$$

while for the contribution coming from diagram in Fig. 3b), in terms of Feynman parametritation method, reads

$$a_\mu = \frac{m_\mu}{8\pi^2}\int_0^1 \frac{2m_\mu(x-1)x}{m_\phi^2 - m_\mu^2 x}. \tag{11}$$

There are also Barr-Zee two-loop contributions to the μAMDM. The dominant contribution is given by

$$a_\mu^{\text{two-loop}} = \frac{\alpha^2}{8\pi^2 s_W^2}\frac{m_\mu^2 g_{A\mu\mu}}{m_W^2} \times \sum_{f=t,\,\tau,\,b} N_c^f Q_f^2 r_f f(r_f) g_{Af_i\bar{f}_i}, \tag{12}$$

where $r_f = (m_f/m_A)^2$, m_f is the fermion mass, $N_c^f = 1(3)$ for leptons (quarks), Q_f is the electric charge of fermions and g_{Aff} is given by the following Lagrangian

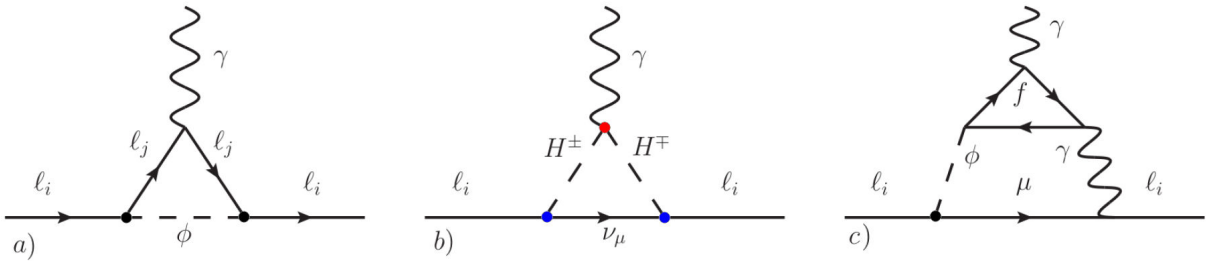

FIGURE 3. Feynman diagrams that contribute to μAMDM. Here ϕ represents a CP-even scalar, CP-odd scalar and the SM-like Higgs boson. $H^\pm$ stand for charged scalar bosons. The μAMM can constrain several free parameters that are function of the $\phi\ell_i\ell_j$, $H^+H^-\gamma$, $H^\pm\ell^\pm\nu_\ell$ interactions, as shown in the black, red and blue circles, respectively. Neutral and/or charged scalar masses $M_{\phi,\,H^\pm}$ ($\phi = H,\ A$) can be also constrained.

$$\mathcal{L} = i\frac{g m_f g_{Aff}}{2m_W}\bar{f}\gamma^5 f A. \tag{13}$$

Finally, the function $f(r_f)$ is given by

$$f(r_f) = \int_0^1 \frac{\log(\frac{r_f}{y(1-y)})}{r_f - y(1-r_f)} dy. \tag{14}$$

2.2.4. *Decays $\ell_i \to \ell_j \ell_k \bar{\ell}_k$*

These types of decays can occur at tree-level via the exchange of scalars changing flavor[ii], as shown in Fig. 4. Nevertheless, the process could be suppressed by the flavor violating Yukawa couplings $Y_{\ell_i \ell_j}$ and by the flavor-conserving coupling $Y_{\ell_k \ell_k}$. However, it depends on the model under consideration.

The decay width is given by

$$\Gamma(\ell_i \to \ell_j \ell_k \bar{\ell}_k) = \sum_{\phi=h,\,H,\,A} \frac{5 m_{\ell_i}^5 |g_{\phi \ell_k \bar{\ell}_k}|^2 (|g_{\phi \ell_j \ell_k}|^2 + |g_{\phi \ell_k \ell_j}|^2)}{24(8\pi)^3 m_\phi^4}. \tag{15}$$

2.2.5. *Decays $B_s^0 \to \mu^+\mu^-$ and $B_d^0 \to \mu^+\mu^-$*

Decays of neutral mesons into muons are strongly suppressed in the theoretical framework of the SM. This suppression arises due to three key factors: (i) they occur through loop diagrams, which are inherently weaker than tree-level processes; (ii) helicity suppression reduces the probability of the interaction; and (iii) the small values of certain CKM matrix elements further diminish the decay rate. Consequently, the branching ratios for these decays are extremely low. While other channels such as electron and τ decays might be theoretically possible, they are strongly suppressed and difficult to reconstruct, respectively. A representative Feynman diagram illustrating this process is shown in Fig. 5.

$B_{s,d}^0$ meson decay into $\mu^+\mu^-$ pair is both interesting and stringent due to its sensitivity to constrain BSM theories. Within the theoretical framework of the SM, the branching ratios are $\mathcal{BR}(B_s^0 \to \mu^+\mu^-) = (3.66 \pm 0.14) \times 10^{-9}$ and $\mathcal{BR}(B_d^0 \to \mu^+\mu^-) = (1.03 \pm 0.05) \times 10^{-10}$ [27], while the current experimental values reported by CMS collaboration

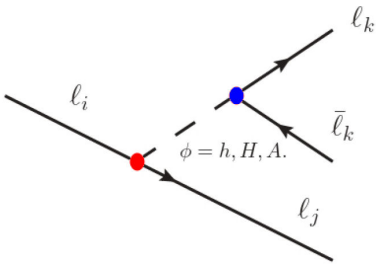

FIGURE 4. Feynman diagrams that contribute to the decay $\ell_i \to \ell_j \ell_k \bar{\ell}_k$. These processes can constrain parameters that are a function of the $\phi \ell_i \ell_j$ and $\phi \ell_k \bar{\ell}_k$ interactions, red and blue circles, respectively.

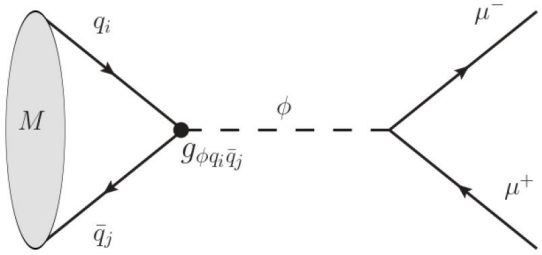

FIGURE 5. Generic Feynman diagram for the decays $M \to \mu^+\mu^-$. The black circle denotes a flavor-changing in the quark sector. Parameters that arise in the $\phi q_i \bar{q}_i$ interactions can be constrained. For the particular case of the decay $B_s^0 \to \mu^-\mu^+$, the parameter to be constrained comes from the $\phi b\bar{s}$ interaction.

are $\mathcal{BR}(B_s^0 \to \mu^+\mu^-) = (4.02^{+0.40}_{-0.38}(\text{stat})^{+0.28}_{-0.23}(\text{syst})^{+0.18}_{-0.15}(B)) \times 10^{-9}$ and $\mathcal{BR}(B_d^0 \to \mu^+\mu^-) < 1.9 \times 10^{-10}$ at 95% C.L. [28], respectively. In the context of the 2HDM-III, the decays $B_{s,d}^0 \to \mu^+\mu^-$ are mediated by the SM-like Higgs boson, the heavy scalar H and the pseudoscalar A and it can arise at tree level. For the decay $B_s^0 \to \mu^+\mu^-$, $q_i = s$ and $\bar{q}_j = \bar{b}$, while for the process $B_d^0 \to \mu^+\mu^-$, $q_i = d$ and $\bar{q}_j = \bar{b}$.

The effective Hamiltonian governing the transition $B_s^0 \to \mu^+\mu^-$ is

$$\begin{aligned}\mathcal{H}_{\text{eff}}^{B_s^0 \to \mu^+\mu^-} = -\frac{G_F^2 m_W^2}{\pi^2}\Big(&C_A^{bs}\mathcal{O}_A^{bs} + C_S^{bs}\mathcal{O}_S^{bs} \\ &+ C_P^{bs}\mathcal{O}_P^{bs} + C_A'^{bs}\mathcal{O}_A'^{bs} \\ &+ C_S'^{bs}\mathcal{O}_S'^{bs} + C_P'^{bs}\mathcal{O}_P'^{bs}\Big) + h.c.,\end{aligned} \tag{16}$$

where the Wilson operators are given as follows

$$\begin{aligned}\mathcal{O}_A^{bs} &= \left(\bar{b}\gamma_\mu P_L s\right)\left(\mu^+\gamma_\mu\gamma_5\mu^-\right), \\ \mathcal{O}_S^{bs} &= \left(\bar{b}P_L s\right)\left(\mu^+\mu^-\right), \\ \mathcal{O}_P^{bs} &= \left(\bar{b}P_L s\right)\left(\mu^+\gamma_5\mu^-\right).\end{aligned} \tag{17}$$

The primed operators are obtained replacing $P_L \leftrightarrows P_R$. The branching ratio for this decay is given by

$$\begin{aligned}\mathcal{BR}\left(M \to \ell^+\ell^-\right) = \frac{G_F^4 m_W^4}{8\pi^5}\sqrt{1 - 4\frac{m_\ell^2}{m_M^2}}\, m_M f_M^2 m_\ell^2 \tau_M \\ \times \Bigg[\left|\frac{m_M^2\left(C_P^{ij} - C_P'^{ij}\right)}{2\left(m_i + m_j\right)m_\ell} - C_A^{\text{SM}}\right|^2 \\ + \left|\frac{m_M^2\left(C_S^{ij} - C_S'^{ij}\right)}{2\left(m_i + m_j\right)m_\ell}\right|^2 \left(1 - 4\frac{m_\ell^2}{m_M^2}\right)\Bigg],\end{aligned} \tag{18}$$

$$C_S^{ij} = \frac{\pi^2}{2G_F^2 m_W^2} \sum_{\phi=h,H} \frac{2g_{\phi\ell^+\ell^-} g_{\phi ij}}{M_\phi^2},$$

$$C_P^{ij} = \frac{\pi^2}{2G_F^2 m_W^2} \frac{2g_{\phi\ell^+\ell^-} g_{\phi ij}}{M_A^2},$$

$$C_S'^{ij} = C_S^{ij}\left(g_{\phi ij} \leftrightarrows g_{\phi ji}\right),$$

$$C_P'^{ij} = C_S^{ij}\left(g_{\phi ij} \leftrightarrows g_{\phi ji}\right), \tag{19}$$

where $\ell^{+(-)} = \mu^{+(-)}$, $i = s$, $j = \bar{b}$, $m_M = m_{B_s^0} = 5.36692$ GeV is the B_s^0 meson mass, $f_M = f_{B_s^0} = 0.2303$ is the B_s^0 meson decay constant, $\tau_M = \tau_{B_s^0} = 2.311 \times 10^{12}$ GeV is the lifetime of the B_s^0 meson, G_F the Fermi constant and the SM contribution at one loop $C_A^{\rm SM}$ is given by

$$C_A^{\rm SM} = -V_{tb}^* V_{ts} Y\left(\frac{m_t^2}{m_W^2}\right) - V_{cb}^* V_{cs} Y\left(\frac{m_c^2}{m_W^2}\right), \tag{20}$$

where the function Y is defined as $Y = \eta_Y Y_0$ such that the NLO QCD effects are included in $\eta_Y = 1.0113$ [29] and the loop Inami-Lim function [30] reads

$$Y_0(x) = \frac{x}{8}\left[\frac{4-x}{1-x} + \frac{3x}{(1-x)^2}\ln(x)\right]. \tag{21}$$

To obtain the corresponding $\mathcal{BR}(B_d^0 \to \mu^+\mu^-)$ we carry out in Eq. (18) the replacements $m_{B_s^0} \to m_{B_d^0} = 5.27966$ GeV, $f_{B_s^0} \to f_{B_d^0} = 0.190$, $\tau_{B_s^0} \to \tau_{B_d^0} = 2.312 \times 10^{12}$ GeV; In Eqs. (19) $g_{\phi\bar{b}s} \to g_{\phi\bar{b}d}$ and in Eqs. (17) $s \to d$.

3. Installation and first steps

3.1. Installation

Run the following instructions in a Notebook of Mathematica

```
In[1]:= Import["https://raw.githubusercontent.
        com/spacemathapp/SpaceMath-v.2.0/alph
        a/Install.m"]
        InstallSpaceMath[]
```

Note that an error may appear because the quotation marks (””); this can be resolved by deleting and then explicitly writing both quotation marks.

Periodically, the SpaceMath package is updated according to new state-of-the-art information, ensuring that the user has access to this updated data simply by executing the following instruction:

```
In[2]:= UpdateSpaceMathData[]
```

To delete SpaceMath automatically, the user only has to execute the following instruction:

```
In[3]:= DeleteSpaceMath[]
```

3.2. First steps

Firts of all, we define in Table III the arguments that are commons in the most commands described below. Thus, we encourage the reader to become familiar with them.

It is important to mention that the LHC option corresponds to measurements done by the Large Hadron Collider (LHC), meanwhile the HE and HL options stand for projections reported in Ref. [31].

3.3. Signal strengths

To generate random points in accordance with experimental measurements, we use the following instructions.

Signal strengths: $\mathcal{R}_b$ & $\mathcal{R}_\tau$

```
In[4]:= Rb[ghtt,ghbb,x1,x1min,x1max,x1label,
        ...,x10,x10min,x10max,x10label,NN]
In[5]:= Rtau[ghtt,ghbb,ghtautau,x1,x1min,x1max,
        x1label,...,x10,x10min,x10max,x10label,NN]
```

TABLE III. Description of arguments shared in all SpaceMath v.2.0 commands.

Argument	Description
xi, (i=1,...,10)	Parameters to constraint
ximin (ximax)	Initial (final) value of the interval to evaluates
xilabel	Label the column i=1,...,10 to be plotted
NN	Random values to generate
ghXX	Represents the g_{hXX} coupling, where XX= $b\bar{b}, t\bar{t}, \tau^-\tau^+, \mu^-\mu^+, e^-e^+, WW, ZZ$
ghXY	Represents the g_{hXY} coupling, where XY= $\mu e, \tau\mu, \tau e$
gAXX	Represents the g_{AXX} coupling, where XX= $b\bar{b}, t\bar{t}, \tau^-\tau^+, \mu^-\mu^+, e^-e^+$
gAXY	Represents the g_{AXY} coupling, where XY= $\mu e, \tau\mu, \tau e$
gHXX	Represents the g_{HXX} coupling, where XX= $b\bar{b}, t\bar{t}, \tau^-\tau^+, \mu^-\mu^+, e^-e^+$
gHXY	Represents the g_{HXY} coupling, where XY= $\mu e, \tau\mu, \tau e$
colliderType	Options: LHC, HE and HL

Signal strengths: $\mathcal{R}_V$, ($V = Z, W$) & $\mathcal{R}_\gamma$

```
In[6]:= RV[ghtt,ghbb,ghVV,x1,x1min,x1max,x1label,...,
        x10,x10min,x10max,x10label,NN]
In[7]:= Rgam[ghtt,ghbb,ghWW,gCH,mCH,x1,x1min,x1max,
        x1label,...,x10,x10min,x10max,x10label,NN]
```

All the signal strengths $\mathcal{R}_X$ & their intersection

```
In[8]:= RALL[ghtt,ghbb,ghZZ,ghWW,ghtautau,gCH,mCH,
        x1,x1min,x1max,x1label,...,x10,x10min,
        x10max,x10label,NN]
In[9]:= Rintersection[ghtt,ghbb,ghZZ,ghWW,ghtautau,
        gCH,mCH,x1,x1min,x1max,x1label,...,
        x10,x10min,x10max,x10label,NN]
```

Here, the `RALL` command includes all the $\mathcal{R}_X$'s to be plotted in a same plot while the instruction `Rintersection` generates random points that satisfy all the $\mathcal{R}_X$'s. In `Rgam`, `RALL` and `Rintersection`, the arguments `gCH` and `mCH` stand for the $g_{hH^+H^-}$ coupling and the mass of a charged scalar boson, respectively, these parameters could come from an extension of the SM. All the points that satisfy the experimental restrictions will be exported to `$UserDocumentDirectory`[iii] (Documents) in a CSV file with the same command's name.

`SpaceMath v.2.0` has its own command to graph the $\mathcal{R}_X$'s. After random points generation, it can accomplished with the following instruction:

```
In[10]:= PlotRX[x1label,...,x10label]
```

The user can generates a particular case of `PlotRX` with the replacement `X` → `b, tau, W, Z, gam, ALL, intersection` for generates the correponding graph for $\mathcal{R}_b$, $\mathcal{R}_\tau$, $\mathcal{R}_W$, $\mathcal{R}_Z$, $\mathcal{R}_\gamma$, $\mathcal{R}_{\rm ALL}$, $\mathcal{R}_{\rm intersection}$, respectively.

Once the main commands have been defined, we focus on the particular case of $\mathcal{R}_{\rm ALL}$, which generates points including all the $\mathcal{R}_X$'s. For this purpose, we consider the Yukawa Lagrangian of the Two-Higgs Doublet Model of type III [32–43], it is given by

$$
\begin{aligned}
\mathcal{L}_Y^{\text{THDM-III}} &= \frac{g}{2}\left(\frac{m_\ell}{m_W}\right)\bar{\ell}_i\left[\frac{\cos\alpha}{\cos\beta}\delta_{ij}+\frac{\sqrt{2}\sin(\alpha-\beta)}{g\cos\beta}\left(\frac{m_W}{m_\ell}\right)\left(\frac{\sqrt{m_i m_j}}{v}\chi_{ij}\right)\right]\ell_j H \\
&+\frac{g}{2}\left(\frac{m_\ell}{m_W}\right)\bar{\ell}_i\left[-\frac{\sin\alpha}{\cos\beta}\delta_{ij}+\frac{\sqrt{2}\cos(\alpha-\beta)}{g\cos\beta}\left(\frac{m_W}{m_\ell}\right)\left(\frac{\sqrt{m_i m_j}}{v}\chi_{ij}\right)\right]\ell_j h \\
&+i\frac{g}{2}\left(\frac{m_\ell}{m_W}\right)\bar{\ell}_i\left[-\tan\beta\delta_{ij}+\frac{\sqrt{2}}{g\cos\beta}\left(\frac{m_W}{m_\ell}\right)\left(\frac{\sqrt{m_i m_j}}{v}\chi_{ij}\right)\right]\gamma^5\ell_j A \\
&+\frac{g}{2}\left(\frac{m_u}{m_W}\right)\bar{u}_i\left[\frac{\sin\alpha}{\sin\beta}\delta_{ij}-\frac{\sqrt{2}\sin(\alpha-\beta)}{g\sin\beta}\left(\frac{m_W}{m_u}\right)\left(\frac{\sqrt{m_i m_j}}{v}\chi_{ij}\right)\right]u_j H \\
&+\frac{g}{2}\left(\frac{m_u}{m_W}\right)\bar{u}_i\left[\frac{\cos\alpha}{\sin\beta}\delta_{ij}-\frac{\sqrt{2}\cos(\alpha-\beta)}{g\sin\beta}\left(\frac{m_W}{m_u}\right)\left(\frac{\sqrt{m_i m_j}}{v}\chi_{ij}\right)\right]u_j h \\
&+i\frac{g}{2}\left(\frac{m_u}{m_W}\right)\bar{u}_i\left[-\cot\beta\delta_{ij}+\frac{\sqrt{2}}{g\sin\beta}\left(\frac{m_W}{m_u}\right)\left(\frac{\sqrt{m_i m_j}}{v}\chi_{ij}\right)\right]\gamma^5 u_j A,
\end{aligned}
\tag{22}
$$

where i and j stand for the fermion flavors, with $i \neq j$, in general. As far as the type-down quark interactions, it is similar to lepton part with the exchange $\ell \to d$ and $m_\ell \to m_d$. In addition to the SM-like Higgs boson, represented by h, the THDM-III predicts two neutral spin-0 particles denoted by H and A in Eq. (22)[iv]

`SpaceMath` offers a collection of pre-loaded notebooks for each previously described observable, then users could implement their models in a quick and easy way.

We start the implementation of THDM-III in `SpaceMath` by executing the RALL and Rintersection commands.

The explicit steps are listed below.

1. Open a notebook of `Mathematica` and load `SpaceMath v.2.0` by typing:

```
In[11]:= <<SpaceMath`
```

2. Select the option `Observables` → `LHC Higgs boson data` → `Signal strength modifiers Rx` → `RALL` and a notebook will be displayed (See Fig. 6). Define the couplings as a function of the parameters to be constrained. In the theoretical framework of THDM-III [Eq. (22)], it is given as follows:

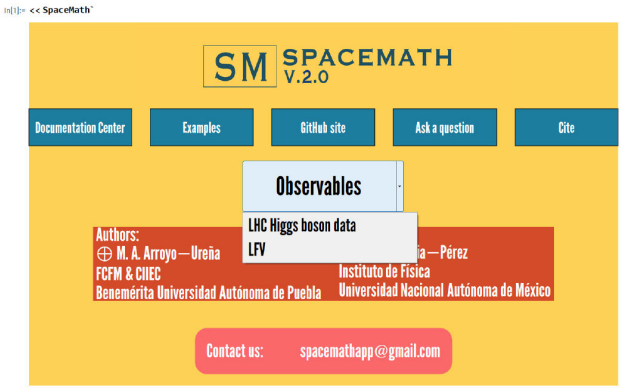

FIGURE 6. SpaceMath package loaded in Mathematica with the **Observables** menu displayed.

```
In[12]:= ghtt[Cab_,tanBeta_,CHItt_]:=(g/2)*(mt/mW)
         *((Cos[ArcCos[Cab]+ArcTan[tanBeta]]/(tan
         Beta*Cos[ArcTan[tanBeta]]))-((Sqrt[2]*Cab)
         /(g*tanBeta*Cos[ArcTan[tanBeta]]))*(mW/vev)
         *CHItt)

In[13]:= ghbb[Cab_,tanBeta_,CHIbb_]:=(g/2)*(mb/mW)
         *((-(Sin[ArcCos[Cab]+ArcTan[tanBeta]]*tan
         Beta)/(Sin[ArcTan[tanBeta]]))+((Sqrt[2]*
         Cab*tanBeta)/(g*Sin[ArcTan[tanBeta]]))*
         (mW/vev)*CHIbb)

In[14]:= ghtautau[Cab_,tanBeta_,CHItautau_]:=(g/2)
         *(mtau/mW)*((-(Sin[ArcCos[Cab]+ArcTan[
         tanBeta]]*tanBeta)/(Sin[ArcTan[tanBeta]])
         )+((Sqrt[2]*Cab*tanBeta)/(g*Sin[ArcTan[
         tanBeta]]))*(mW/vev)*CHItautau)

In[15]:= ghWW[Cab_]:=gw*mW*Sqrt[1-Cab^2]

In[16]:= ghZZ[Cab_]:=gz*mZ*Sqrt[1-Cab^2]

In[17]:= gCH[Cab_,tanBeta_]:=(mW*Sin[ArcTan[tanBeta]
         -(ArcCos[Cab]+ArcTan[tanBeta])]+mZ
         /(2*CW)*Cos[2 ArcTan[tanBeta]]*Sin[ArcTan[tan
         Beta]+(ArcCos[Cab]+ArcTan[tanBeta])])*g
```

where Cab, tanBeta, CHItt and CHIbb are identified with $\cos(\alpha-\beta)$, $\tan\beta$, χ_{tt}, χ_{bb}, respectively. The complete list of couplings can be found in Appendix A.

3. Later, we execute the instruction

```
In[18]:= RALL[
             ghtt[Cab, tanBeta, CHItt],
             ghbb[Cab, tanBeta, CHIbb],
             ghZZ[Cab],
             ghWW[Cab],
             ghtautau[Cab, tanBeta, CHItautau],
             gCH[Cab, tanBeta],
             mCH,
             Cab, -1, 1, "Cab",
             tanBeta, 0, 50, "tanBeta",
             CHItt, -850, 850, "CHItt",
             CHIbb, -1, 1, "CHIbb",
             CHItautau, -1, 1, "CHItautau",
             mCH, 100, 1000, "mCH",
             x7, 0, 0, " ",
             x8, 0, 0, " ",
             x9, 0, 0, " ",
             x10, 0, 0, " ",
             1000000
             ];
```

4. Once the random points have been generated (point 3), in this case we considered NN=1000000, the command to plot them is the following:

```
In[19]:= PlotRALL["cos(α-β)","tanβ","χtt",
         "χbb","χττ","mH±","","","","",""];
```

where *x1label*="$\cos(\alpha-\beta)$", *x2label*="$\tan\beta$", *x3label*="χ_{tt}", *x4label*="χ_{bb}", *x5label*="$\chi_{\tau\tau}$",

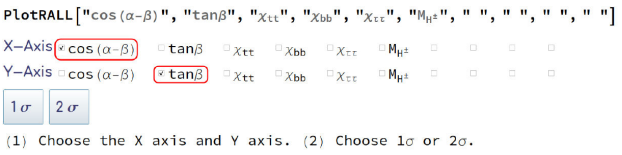

FIGURE 7. In this menu the user select the plane to be plotted. In this particular case, the parameters $\cos(\alpha-\beta)$ and $\tan\beta$ have been selected by clicking.

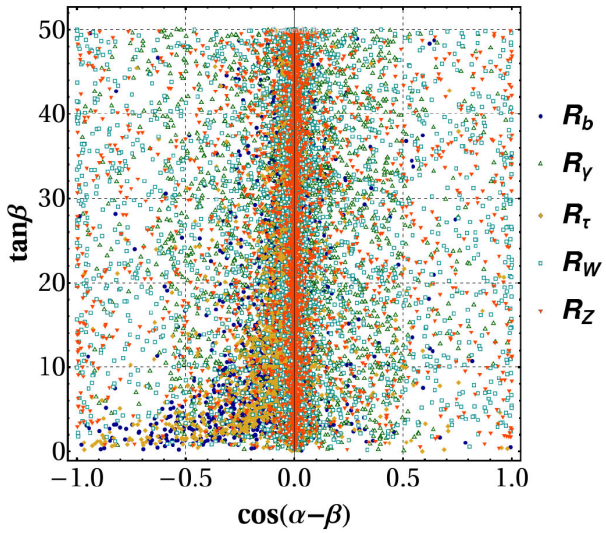

FIGURE 8. Plot generated by SpaceMath v.2.0 via the command PlotRALL. Points orange (purple, green, red and blue) are the ones that satisfy $\mathcal{R}_b$ ($\mathcal{R}_\gamma$, $\mathcal{R}_\tau$, $\mathcal{R}_W$ and $\mathcal{R}_Z$).

`x6label`="$m_{H^\pm}$". Notice that in `PlotRALL` the arguments are enclosed in quotes ("...").

After executing the instruction `PlotRALL[...]`, a menu will be displayed. If the user has selected the checkboxes as shown in Fig. 7, then the Fig. 8 will be generated.

Machine learning

We have implemented methods of machine learning in `SpaceMath v.2.0` to generate specific Benchmark Points useful to evaluate the calculations of physical observables of interest.

`SpaceMath v.2.0` through the Wolfram Language offers fully automated and highly customizable machine learning functions to perform predictions from data through the `Predict`^{v} command as follows:

`Predict[Data, input]`→ attempts to predict the output associated with input from the training examples given. `Data` are imported from the `SpaceMath v.2.0` commands: `Rintersection[...]`, `Rintersection[...]` and `LFVintersection[...]`, as shown later.

There are different Machine Learning methods [44–46] to be used along with the command `Predict`. In all the cases, `Ralgorithm`, `Kalgorithm`, `LFValgorithm`, invokes the database created by `Rintersection`, `Kintersection`, `LFVintersection`, respectively. Here `algorithm` stands for the Machine Learning method used to predict. `SpaceMath v.2.0` implements five of them:

1. `Linear Regression:` This method models relationships between predictive parameters and experimental constraints through linear combinations. In `SpaceMath`, Linear Regression is implemented using the `RLinearRegression`, `KLinearRegression` and `LFVLinearRegression` commands. It serves as an initial tool to identify linear correlations between the parameters, simplifying the early stages of analysis.

2. `Neural Networks:` This algorithm is invoked via the `RNeuralNetworks`, `KNeuralNetworks` and `LFVNeuralNetworks` commands. Its function is to model highly nonlinear relationships and intricate patterns in the parameter space.

3. `Decision Trees:` This method partition the parameter space into hierarchical regions based on decision rules derived from the data. To run this algorithm, use the `RDecisionTrees`, `KDecisionTrees` and `LFVDecisionTrees` commands.

4. `Gradient Boosted Trees:` This models combine multiple decision trees to minimize prediction errors, making them effective for problems with complex relationships. The corresponding `SpaceMath` commands are `RGradientBoostedTrees`, `KGradientBoostedTrees` and `LFVGradientBoostedTrees`.

5. `Gaussian Processes:` This probabilistic approach captures uncertainties in predictions and is ideal for limited data or nonlinear relationships. It is implemented via `RGaussianProcess`, `KGaussianProcess` and `LFVGaussianProcess`, enabling the extrapolation of parameter values into unexplored regions.

To use the previous Machine Learning methods we again consider the interactions from Eq. (22) and we execute the instruction `Rintersection`, as follows:

```
In[20]:= Rintersection[
         ghtt[Cab, tanBeta, CHItt],
         ghbb[Cab, tanBeta, CHIbb],
         ghZZ[Cab],
         ghWW[Cab] ,
         ghtautau[Cab, tanBeta, CHItautau],
         gCH[Cab, tanBeta],
         mCH,
         Cab, -1, 1, "Cab",
         tanBeta, 0, 50, "tanBeta",
         CHItt, -850, 850, "CHItt",
         CHIbb, -1, 1, "CHIbb",
         CHItautau, -1, 1, "CHItautau",
         mCH, 100, 1000, "mCH",
         x7, 0, 0, " ",
         x8, 0, 0, " ",
         x9, 0, 0, " ",
         x10, 0, 0, " ",
         100000000
         ];
```

To plot the points generated via the command `Rintersection[...]` the user can use the instruction:

```
In[21]:= PlotRintersection["cos(α-β)","tanβ",
         "χtt","χbb","χττ","mH±","","","","",""]
```

whose output will be a graph as shown in Fig. 9.

Once the user has generated the random points, the command that involke these algorithms is as follows.

```
In[22]:= Ralgorithm[x1label,...,x10label]
```

where `algorithm` → `LinearRegression`, `DecisionTrees`, `GaussianProcess`, `GradientBoostedTrees`, `NeuralNetworks`.

We suggest using `Rintersection` as this considers the points that pass the test of all $\mathcal{R}_X$'s. In this way, in order to illustrate how `SpaceMath v.2.0` works, we consider `Rintersection` applied to the THDM-III:

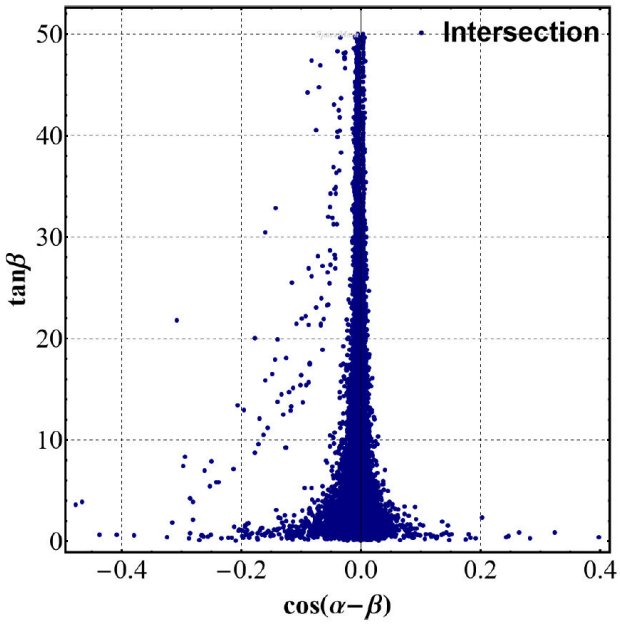

FIGURE 9. Plot generated by SpaceMath v.2.0 via the command PlotRintersection. The blue points stand for these allowed by all the $\mathcal{R}_X$'s defined in Eq. (1).

```
In[23]:= RLinearRegression["cos(α-β)","tanβ",
         "χtt","χbb","χττ","mH±","","","","",""]

In[24]:= RDecisionTrees["cos(α-β)","tanβ",
         "χtt","χbb","χττ","mH±","","","","",""]

In[25]:= RGradientBoostedTrees["cos(α-β)","tanβ",
         "χtt","χbb","χττ","mH±","","","","",""]

In[26]:= RNeuralNetworks["cos(α-β)","tanβ","χtt",
         "χbb","χττ","mH±","","","","",""]

In[27]:= RGaussianProcess["cos(α-β)","tanβ",
         "χtt","χbb","χττ","mH±","","","","",""]
```

Note that the parameters to be predicted must be enclosed in quotation marks. If the analysis is for fewer than ten parameters, only the quotation marks must be used in the remaining entries.

TABLE IV. Benchmark Points predicted by the Machine Learning methods.

Method	$\cos(\alpha-\beta)$	$\tan\beta$	χ_{tt}	χ_{bb}	$\chi_{\tau\tau}$	$m_{H^\pm}$
Linear Regression	−0.007	12.94	170.26	0.104	0.124	551.67
Decision Trees	−0.007	13.13	169.91	0.119	0.115	551.73
Gradiant Boosted Trees	−0.007	13.43	216.22	0.088	0.065	564.74
Neural Networks	−0.005	12.67	104.72	0.099	0.153	586.01

The SpaceMath v.2.0 predictions are given in Table IV.

Higgs boson coupling modifiers κ_i

On the other hand, the Higgs boson coupling modifiers κ_i, as defined in Sec. 2.1.2 include the following commands:

Higgs boson coupling modifiers: $\mathcal{K}_b$ & $\mathcal{K}_\tau$

```
In[28]:= Kb[ghbb,x1,x1min,x1max,x1label,...,x10,
         x10min,x10max,x10label,NN,colliderType]

In[29]:= Ktau[ghtautau,x1,x1min,x1max,x1label,
         ...,x10,x10min,x10max,x10label,NN,
         colliderType]
```

Higgs boson coupling modifiers: $\mathcal{K}_V$, ($V = Z, W$) & $\mathcal{K}_\gamma$

```
In[30]:= KV[ghVV,x1,x1min,x1max,x1label,...,x10,x10min,x10max,x10label,NN,colliderType]

In[31]:= Kgam[ghtt,ghbb,ghWW,gCH,mCH,x1,x1min,
         x1max,x1label,...,x10,x10min,x10max,
         x10label,NN,colliderType]
```

Higgs boson coupling modifiers $\mathcal{K}_g$

```
In[32]:= Kglu[ghtt,ghbb,x1,x1min,x1max,x1label,
         ...,x10,x10min,x10max,x10label,NN,
         colliderType]
```

All the Higgs boson coupling modifiers $\mathcal{K}_X$ & their intersection

```
In[33]:= KALL[ghtt,ghbb,ghZZ,ghWW,ghtautau,gCH,
         mCH,x1,x1min,x1max,x1label,...,x10,
         x10min,x10max,x10label,NN,colliderType]

In[34]:= Kintersection[ghtt,ghbb,ghZZ,ghWW,ghtautau,
         gCH,mCH,x1,x1min,x1max,x1label,...,x10,
         x10min,x10max,x10label,NN,colliderType]

In[35]:= PlotKX[x1label,...,x10label,colliderType]
```

Note the last entry of all commands: colliderType=LHC, HL, HE. If the user selects LHC, then SpaceMath V.2.0 considers results reported by the LHC, while the HL or HE option takes into account projections expected at the High-Luminosity LHC or High-Energy LHC, respectively.

Machine learning

```
In[36]:= Kalgorithm[x1label,...,x10label,
         colliderType]
```

We continue the implementation of the THDM-III by executing the commands KALL, Kintersection, and Kalgorithms. The way to proceed is similar to the previous one presented in Subsec. 3.3.

```
In[37]:= KALL[
         ghtt[Cab, tanBeta, CHItt],
         ghbb[Cab, tanBeta, CHIbb],
         ghZZ[Cab],
         ghWW[Cab] ,
         ghtautau[Cab, tanBeta, CHItautau],
         gCH[Cab, tanBeta],
         mCH,
         Cab, -1, 1, "Cab",
         tanBeta, 0, 50, "tanBeta",
         CHItt, -850, 850, "CHItt",
         CHIbb, -1, 1, "CHIbb",
         CHItautau, -1, 1, "CHItautau",
         mCH, 100, 1000, "mCH",
         x7, 0, 0, " ",
         x8, 0, 0, " ",
         x9, 0, 0, " ",
         x10, 0, 0, " ",
         5000,
         "LHC"
         ];

In[38]:= Kintersection[
         ghtt[Cab, tanBeta, CHItt],
         ghbb[Cab, tanBeta, CHIbb],
         ghZZ[Cab],
         ghWW[Cab] ,
         ghtautau[Cab, tanBeta, CHItautau],
         gCH[Cab, tanBeta],
         mCH,
         Cab, -1, 1, "Cab",
         tanBeta, 0, 50, "tanBeta",
         CHItt, -850, 850, "CHItt",
         CHIbb, -1, 1, "CHIbb",
         CHItautau, -1, 1, "CHItautau",
         mCH, 100, 1000, "mCH",
         x7, 0, 0, " ",
         x8, 0, 0, " ",
         x9, 0, 0, " ",
         x10, 0, 0, " ",
         30000000,
         "LHC"
         ];
```

```
In[39]:= PlotKALL["cos(α-β)","tanβ","χtt","χbb",
         "χττ","mH±","","","","","","LHC"]

In[40]:= PlotKintersection["cos(α-β)","tanβ","χtt",
         "χbb","χττ","mH±","","","","","","LHC"]
```

The graphs generated by the `PlotKALL` and `PlotKintersection` commands are shown in Fig. 10.

Meanwhile, the instruction to generate the Benchmark Points by the different Machine Learning methods are the following:

```
In[41]:= KLinearRegression["cos(α-β)","tanβ",
         "χtt","χbb","χττ","mH±","","","","",""]

In[42]:= KDecisionTrees["cos(α-β)","tanβ","χtt",
         "χbb","χττ","mH±","","","","",""]

In[43]:= KGradientBoostedTrees["cos(α-β)","tanβ",
         "χtt","χbb","χττ","mH±","","","","",""]

In[44]:= KNeuralNetworks["cos(α-β)","tanβ","χtt",
         "χbb","χττ","mH±","","","","",""]

In[45]:= KGaussianProcess["cos(α-β)","tanβ",
         "χtt","χbb","χττ","mH±","","","","",""]
```

The Benchmarck Points found are given in Table V.

Lepton Flavor Violating processes

$h \to \ell_i \ell_j$ decay

The command to generate the parameter space allowed by the upper limit on the $\mathcal{BR}(h \to \ell_i \ell_j)$ is the following:

```
In[46]:= hlilj[ghlilj,x1,x1min,x1max,x1label,...,
         x10,x10min,x10max,x10label,NN]
```

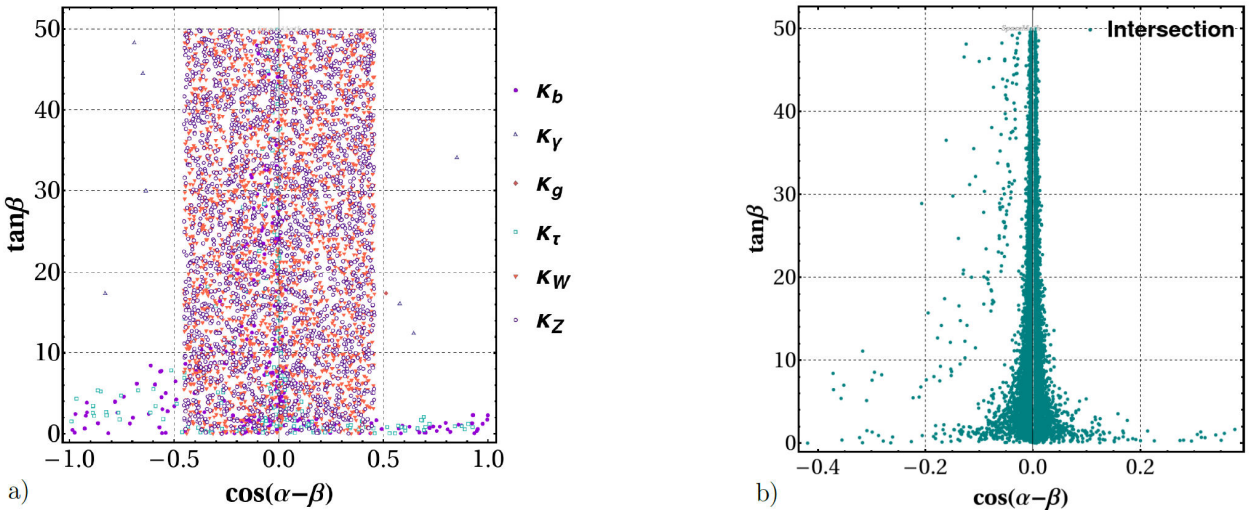

FIGURE 10. Plot generated by `SpaceMath v.2.0` via the commands: a) `PlotKALL`, each point on the graph corresponds to a specific κ_i and represents values that satisfy such a κ_i. b) `PlotKintersection`, the points on that graph are those that satisfy all the κ_i's.

TABLE V. Benchmark Points predicted by the Machine Learning algorithms.

Method	$\cos(\alpha-\beta)$	$\tan\beta$	χ_{tt}	χ_{bb}	$\chi_{\tau\tau}$	$m_{H^\pm}$
Linear Regression	-0.004	15.16	33.61	0.047	0.131	561.68
Decision Trees	-0.003	15.16	32.83	-0.009	-0.041	554.91
Gradiant Boosted Trees	-0.005	12.14	55.63	-0.021	0.007	551.66
Neural Networks	-0.0005	15.64	72.4	0.095	0.141	517.64

where `ghlilj` stands for the $h\ell_i\ell_j$ coupling, while the rest of the parameters are defined in Table III. The command `hlilj` exports an output file with values agree with such an upper limit, its name is labeled as `hlilj.csv` and it will be saved in `$UserDocumentsDirectory`. The command to graph the data generated by `hlilj` is given by

```
In[47]:= Plothlilj[x1label,...,x10label]
```

Assuming the interactions shown in Eq. (22), the `SpaceMath` code (when $\ell_i=\tau$ and $\ell_j=\mu$) is as follows.

```
In[48]:= hTauMu[
         ghtaumu[Cab, tanBeta, CHItaumu],
         Cab, -1, 1, "Cab",
         tanBeta, 0, 50, "tanBeta",
         CHItaumu, -1, 1, "CHItaumu",
         x4, 0, 0, " ",
         x5, 0, 0, " ",
         x6, 0, 0, " ",
         x7, 0, 0, " ",
         x8, 0, 0, " ",
         x9, 0, 0, " ",
         x10, 0, 0, " ",
         100000
         ];
```

where

$$\texttt{ghtaumu[Cab,tanBeta,CHItaumu]} = \frac{\cos(\alpha-\beta)}{\sqrt{2}\cos\beta}\frac{\sqrt{m_\tau m_\mu}}{v}\chi_{\tau\mu} = \frac{\cos(\alpha-\beta)\tan\beta}{\sqrt{2}\sin\beta}\frac{\sqrt{m_\tau m_\mu}}{v}\chi_{\tau\mu}, \quad (23)$$

is the $h\tau\mu$ coupling which depends on the parameters to be constrained. Note that the $h\tau\mu$ coupling depends only on three parameters, `x1=Cab`, `x2=tanBeta`, `x3=CHItaumu`. In this case, the remaining 6 parameters are free, so it is recommended to set their values to 0, that is, `x4min=x4max=0`, `x5min=x5max=0`, `x6min=x6max=0`, `x7min=x7max=0`, `x8min=x8max=0`, `x9min=x9max=0` and `x10min=x10max=0`. Again, to plot the data we use the command `PlothTauMu`.

```
In[49]:= PlothTauMu["cos(α-β)","tanβ","χτμ",
         "","","","","","","","","","",""]
```

Notice that the instruction `Plothlilj` works as the command `PlotRALL`.

Figure 11 shows the plot generated by the command `PlothTauMu`.

$\ell_i \to \ell_j\gamma$ decays

As far as the $\ell_i \to \ell_j\gamma$ decays are concerned, the command to generate the parameter space allowed by current upper bounds on $\mathcal{BR}(\tau\to\mu\gamma)$ (see Table II) is given by:

```
In[50]:= TauMuGamma[ghtaumu,ghtautau,gAtaumu,
         gAtautau,gHtaumu,gHtautau,ghtt,gHtt,
         gAtt,mH,mA,x1,x1min,x1max,x1label,
         ...,x10,x10min,x10max,x10label,NN]
```

The command `TauMuGamma` exports an output file (`TauMuGamma.csv`) to `$UserDocumentsDirectory` with values in accordance with the upper bounds on $\mathcal{BR}(\ell_i\to\ell_j\gamma)$ (see Table II).

To analyze the model parameter space via $\mu\to e\gamma$ users must make replacements

`TauMuGamma` → `MuEGamma`,

`gPHItaumu` → `gPHImue`, `gPHItautau` → `gPHImumu`,

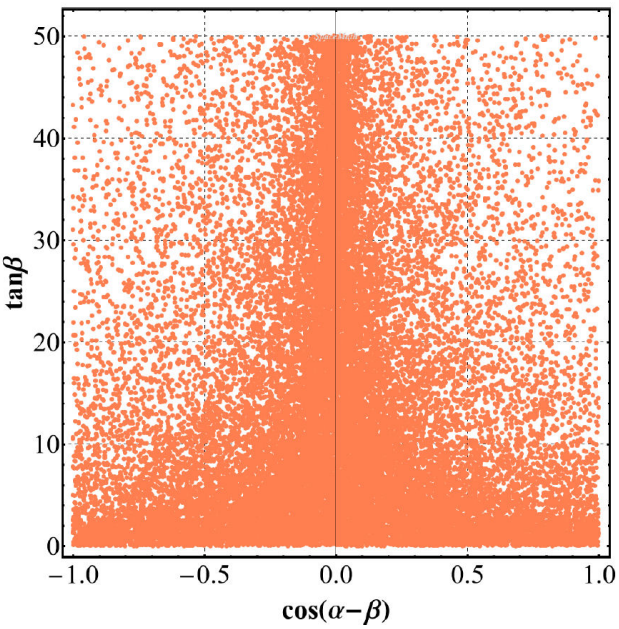

FIGURE 11. Graph generated by `SpaceMath v.2.0` via the instruction in Eq. `PlothTauMu[...]`. The orange points stand for the ones that satisfy the upper limit on $\mathcal{BR}(h\to\tau\mu)$.

where `PHI = h, H, A`. And analogously for the $\tau \to e\gamma$ decay

$$\texttt{TauMuGamma} \to \texttt{TauEGamma},$$

$$\texttt{gPHItaumu} \to \texttt{gPHItaue}.$$

The explicit instruction to constrain the free model parameters via the upper limit on the $\mathcal{BR}(\tau \to \mu\gamma)$ is given by:

```
In[51]:= TauMuGamma[
          ghtaumu[Cab, tanBeta, CHItaumu],
          ghtautau[Cab, tanBeta, CHItautau],
          gAtaumu[tanBeta, CHItaumu],
          gAtautau[tanBeta, CHItautau],
          gHtaumu[Cab, tanBeta, CHItaumu],
          gHtautau[Cab, tanBeta, CHItautau],
          gHtautau[Cab, tanBeta, CHItautau],
          ghtt[Cab, tanBeta, CHItt],
          gHtt[Cab, tanBeta, CHItt],
          gAtt[tanBeta, CHItt],
          mH,
          mA,
          Cab, -1, 1, "Cab",
          tanBeta, 0, 50, "tanBeta",
          CHItaumu, -1, 1, "CHItaumu",
          CHItt, -850, 850, "CHItt",
          CHItautau, -1, 1, "CHItautau",
          mH, 300, 1000, "mH",
          mA, 100, 1000, "mA",
          x8, 0, 0, " ",
          x9, 0, 0, " ",
          x10, 0, 0, " ",
          100000
          ];
```

To generate the corresponding plot of the parameter space we use

```
In[52]:= PlotLiLjGamma[x1label,...,x10label]
```

For the particular case when `Li` $= \tau$ and `Lj` $= \mu$, the specific instruction to follow is

```
In[53]:= PlotTauMuGamma["cos(α-β)","tanβ",
          "χτμ","χtt","χττ","mH","mA","","",""]
```

$\ell_i \to \ell_j \ell_k \bar{\ell}_k$ decays and δa_μ

In order not to overload the user with information, the procedure for analyzing the observables $\ell_i \to \ell_j \ell_k \bar{\ell}_k$ and δa_μ is similar to the previous instructions. User can follow the path as shown in the instructions (24) to consult preloaded examples in `SpaceMath v.2.0`.

Li3Lj[...] : SpaceMath-2.0 → Observables → LFV → Tau3Mu,

muonAMDM[...] : SpaceMath-2.0 → Observables → LFV → muonAMDM. (24)

LFVALL

Finally, we present the instructions to display all the LFV processes in an individual plot as follows:

```
In[54]:= LFVALL[
          ghtaue[Cab, tanBeta, CHItaue],
          ghtaumu[Cab, tanBeta, CHItaumu],
          ghtautau[Cab, tanBeta, CHItautau],
          ghee[Cab, tanBeta, CHIee],
          ghmue[Cab, tanBeta, CHImue],
          ghmumu[Cab, tanBeta, CHImumu],
          gAee[tanBeta, CHIee],
          gAtaue[tanBeta, CHItaue],
          gAtaumu[tanBeta, CHItaumu],
          gAtautau[tanBeta, CHItautau],
          gAmue[tanBeta, CHImue],
          gAmumu[tanBeta, CHImumu],
          gHee[Cab, tanBeta, CHIee],
          gHtaue[Cab, tanBeta, CHItaue],
          gHtaumu[Cab, tanBeta, CHItaumu],
          gHtautau[Cab, tanBeta, CHItautau],
          gHmue[Cab, tanBeta, CHImue],
          gHmumu[Cab, tanBeta, CHImumu],
          ghtt[Cab, tanBeta, CHItt],
          gHtt[Cab, tanBeta, CHItt],
          gAtt[tanBeta, CHItt],
          gHbb[Cab, tanBeta, CHIbb],
          gAbb[tanBeta, CHIbb],
          ghbb[Cab, tanBeta, CHIbb],
          gCHmunmu[tanBeta, CHImumu],
          mH,
          mA,
          mCH,
          Cab, -1, 1, "Cab",
          tanBeta, 0, 50, "tanBeta",
          CHItt, -850, 850, "CHItt",
          CHItaumu, -1, 1, "CHItaumu",
          CHItaue, -1, 1, "CHItaue",
          CHItautau, -1, 1, "CHItautau",
          CHImumu, -1, 1, "CHImumu",
          mH, 300, 1000, "mH",
          mA, 300, 1000, "mA",
          mCH, 100, 1000, "mCH",
          3000
          ];
```

Note that we included the full couplings involved in each individual processes. The command to generate the allowed values by the LFV processes read:

```
In[55]:= PlotLFVALL["cos(α-β)","tanβ","χtt",
          "χτμ","χτ e","χττ","χμμ","mH","mA","mH±"]
```

Figure 13 presents the graph obtained by previuos command `PlotLFVALL[...]`.

LFVintersection

As far as the instersection is concerned, the instruction to archieved it is given by `LFVintersection[...]` as presented below.

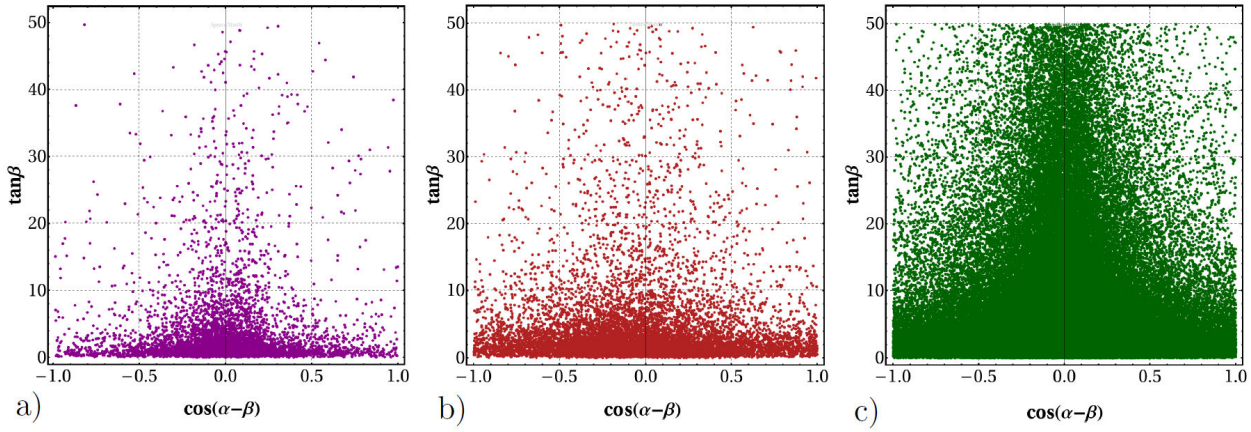

FIGURE 12. Graph generated by SpaceMath v.2.0 via the instruction PlotLiLjGamma: a) PlotTauMuGamma, b) PlotMuEGamma and c) PlotTauEGamma.

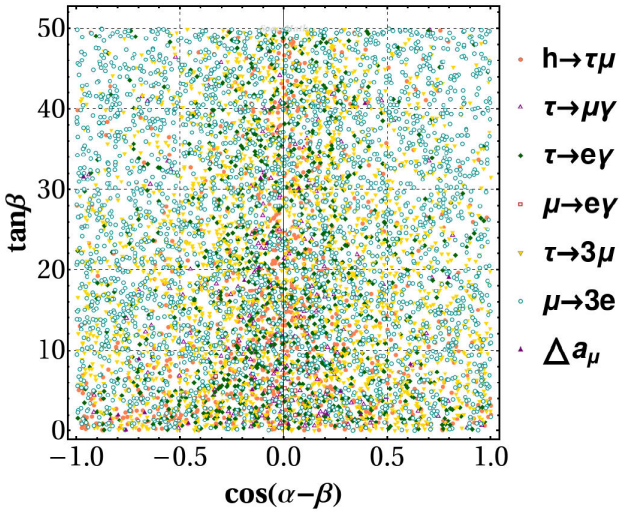

FIGURE 13. Graph generated by SpaceMath v.2.0 via the instruction *PlotLFVALL*.

```
In[56]:= LFVintersection[
           ghtaue[Cab, tanBeta, CHItaue],
           ghtaumu[Cab, tanBeta, CHItaumu],
           ghtautau[Cab, tanBeta, CHItautau],
           ghee[Cab, tanBeta, CHIee],
           ghmue[Cab, tanBeta, CHImue],
           ghmumu[Cab, tanBeta, CHImumu],
           gAee[tanBeta, CHIee],
           gAtaue[tanBeta, CHItaue],
           gAtaumu[tanBeta, CHItaumu],
           gAtautau[tanBeta, CHItautau],
           gAmue[tanBeta, CHImue],
           gAmumu[tanBeta, CHImumu],
           gHee[Cab, tanBeta, CHIee],
           gHtaue[Cab, tanBeta, CHItaue],
           gHtaumu[Cab, tanBeta, CHItaumu],
           gHtautau[Cab, tanBeta, CHItautau],
           gHmue[Cab, tanBeta, CHImue],
           gHmumu[Cab, tanBeta, CHImumu],
           ghtt[Cab, tanBeta, CHItt],
           gHtt[Cab, tanBeta, CHItt],
           gAtt[tanBeta, CHItt],
           gHbb[Cab, tanBeta, CHIbb],
           gAbb[tanBeta, CHIbb],
           ghbb[Cab, tanBeta, CHIbb],
           gCHmunmu[tanBeta, CHImumu],
           mH,
           mA,
           mCH,
           Cab, -1, 1, "Cab",
           tanBeta, 0, 50, "tanBeta",
           CHItt, -850, 850, "CHItt",
           CHItaumu, -1, 1, "CHItaumu",
           CHItaue, -1, 1, "CHItaue",
           CHItautau, -1, 1, "CHItautau",
           CHImumu, -1, 1, "CHImumu",
           mH, 300, 1000, "mH",
           mA, 300, 1000, "mA",
           mCH, 100, 1000, "mCH",
           100000000
           ];
```

Concerning to the command for graph it is

```
In[57]:= PlotLFVintersection["cos(α-β)","tanβ",
           "χtt","χτμ","χτ e","χττ","χμμ","mH","mA",
           "mH±"],
```

whose plot is displayed in Fig. 14.

Meanwhile, the instruction to generate the Benchmark Points by the different Machine Learning methods are the following:

```
In[58]:= LFVLinearRegression["cos(α-β)","tanβ",
           "χtt","χτμ","χτ e","χττ","χμμ","mH","mA",
           "mH±"]

In[59]:= LFVDecisionTrees["cos(α-β)","tanβ","χtt",
           "χτμ","χτ e","χττ","χμμ","mH","mA","mH±"]
```

TABLE VI. Benchmark Points predicted by the Machine Learning algorithms.

Method	$\cos(\alpha-\beta)$	$\tan\beta$	χ_{tt}	$\chi_{\tau\mu}$	$\chi_{\tau e}$
Linear Regression	0.025	6.93	−131.73	0.003	0.016
Decision Trees	0.026	6.93	−129.57	0.003	0.36
Gradiant Boosted Trees	0.028	6.71	−114.33	−0.003	0.032
Neural Networks	0.029	4.3	−110.65	0.02	−0.034
	$\chi_{\tau\tau}$	$\chi_{\mu\mu}$	m_H	m_A	$m_{H^\pm}$
	0.00227802	−0.0134181	772.29	688.825	551.469
	0.00213208	−0.00953442	772.29	688.824	551.427
	−0.0841526	−0.0220177	774.676	700.979	550.757
	0.0078228	−0.0638356	762.177	711.47	547.118

TABLE VII. First column: THDM-I, -II couplings. Second column: coupling defined in `SpaceMath (v(V)=, z(Z), w(W))`. Third column: `SpaceMath` code.

Coupling	Input to SpaceMath	Command κ_i
$g_{hbb}^{THDM-I} = \frac{gm_b}{2m_W}\left(\frac{\cos\alpha}{\sin\beta}\right)$	`ghbb[Sa_,Tb_,Cb_]:` `=g*mb*Sqrt[1-Sa^2]/(2*mW*Tb*Cb)`	`kb[ghbb[Sa,Tb,Cos[ArcTan[Tb]]]]`
$g_{hbb}^{THDM-II} = \frac{gm_b}{2m_W}\left(\frac{-\sin\alpha}{\cos\beta}\right)$	`ghbb[Sa_,Tb_,Sb_]:` `=-g*mb*Sa*Tb/(2*mW*Sb)`	`kb[ghbb[Sa,Tb,Sin[ArcTan[Tb]]]]`
$g_{hVV}^{THDM-I,-II} = g_V m_V \sin(\beta-\alpha)$	ghVV[Tb_,Cb_,Sb_,Sa_]: =((Tb*Cb*Sqrt[1-Sa^2])-(Sb/Tb*Sa))*(gv*mV)	`kV[ghVV[Tb, Cos[ArcTan[Tb]], Sin[ArcTan[Tb]], Sa]]`

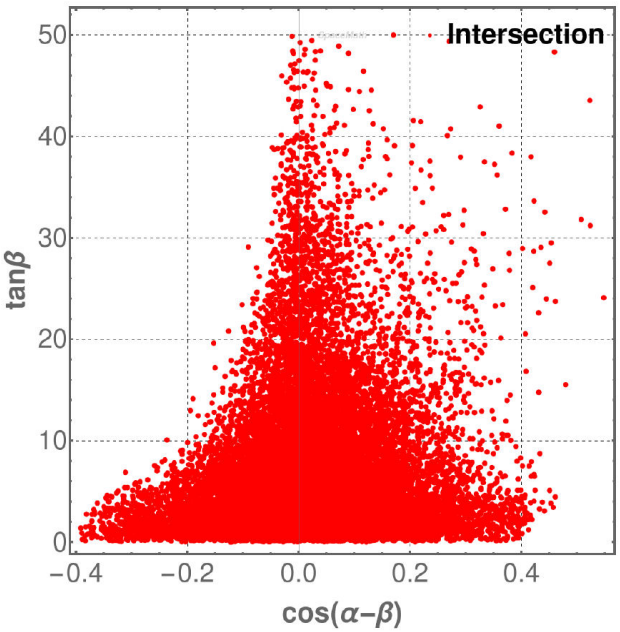

FIGURE 14. Graph generated by `PlotLFVintersection[...]`. The red points are the ones that satisfy all the LFV processes.

```
In[60]:= LFVGradientBoostedTrees["cos(α-β)","tanβ",
         "χtt","χτμ","χτ e","χττ","χμμ","mH",
         "mA","mH±"]
```

```
In[61]:= LFVNeuralNetworks["cos(α-β)","tanβ","χtt",
         "χτμ","χτ e","χττ","χμμ","mH","mA","mH±"]
```

```
In[62]:= LFVGaussianProcess["cos(α-β)","tanβ","χtt",
         "χτμ","χτ e","χττ","χμμ","mH","mA","mH±"]
```

The Benchmarck Points found are given in Table VI.

4. Validation

In order to validate `SpaceMath v.2.0`, we apply the coupling modifiers κ_i defined in Eq. (2) to the Two-Higgs Doublet Model of Type I and II (THDM-I, II). In Ref. [47] are reported κ_b and κ_V in the context of these models. To reproduce these results via `SpaceMath v.2.0` the only we need to know are the model couplings, which are given in Table VIII. The commands to evaluate κ_b and κ_V are displayed in Table VII.

We have defined `Sa`$\equiv\sin\alpha$, `Tb`$\equiv\tan\beta$, `Cb`$\equiv\cos\beta$, `Sb`$\equiv\sin\beta$ are free parameters of THDM-I, -II. In addition, we have used the relations $\tan\beta = \frac{\sin\beta}{\cos\beta}$, $\sin(\beta-\alpha) = \sin\beta\cos\alpha - \cos\beta\sin\alpha$. The commands `kb` and `kV` can be directly evaluated by introducing values for `Sa, Tb, Cb`, or since `SpaceMath` is hosted in `Mathematica`, we can use its commands to graph. For this example we use:

```
In[63]:= ContourPlot[kb[ghbb[Sa,Tb,
         Cos[ArcTan[Tb]]]]^2,{Sa,-1,1},{Tb,0,20}]
```

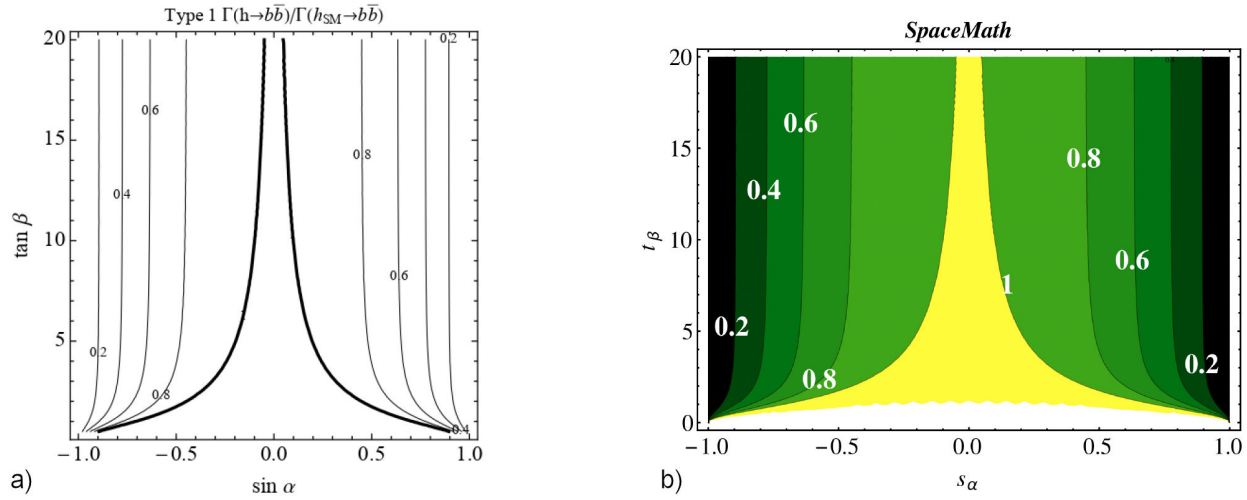

FIGURE 15. Contours of $\Gamma(h \to b\bar{b})/\Gamma(h_{SM} \to b\bar{b})$ for the SM-like Higgs boson as a function of $\sin\alpha$ and $\tan\beta$ in Type 1 THDM. Left: figure taken from [47] and Right: figure generated by `SpaceMath v.2.0`.

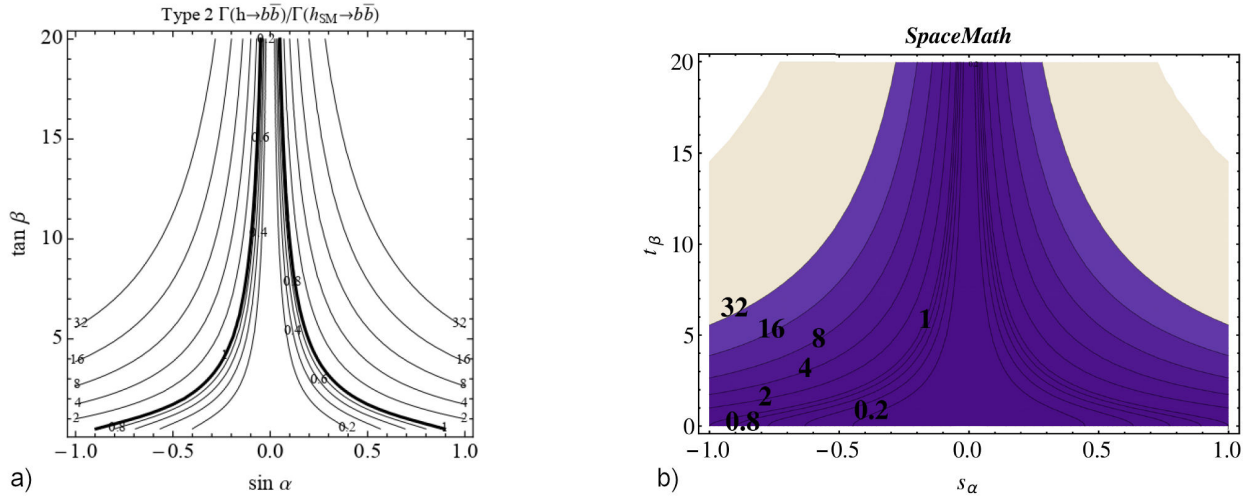

FIGURE 16. Contours of $\Gamma(h \to b\bar{b})/\Gamma(h_{SM} \to b\bar{b})$ for the SM-like Higgs boson as a function of $\sin\alpha$ and $\tan\beta$ in Type 2 THDM. Left: figure taken from [47] and Right: figure generated by `SpaceMath v.2.0`.

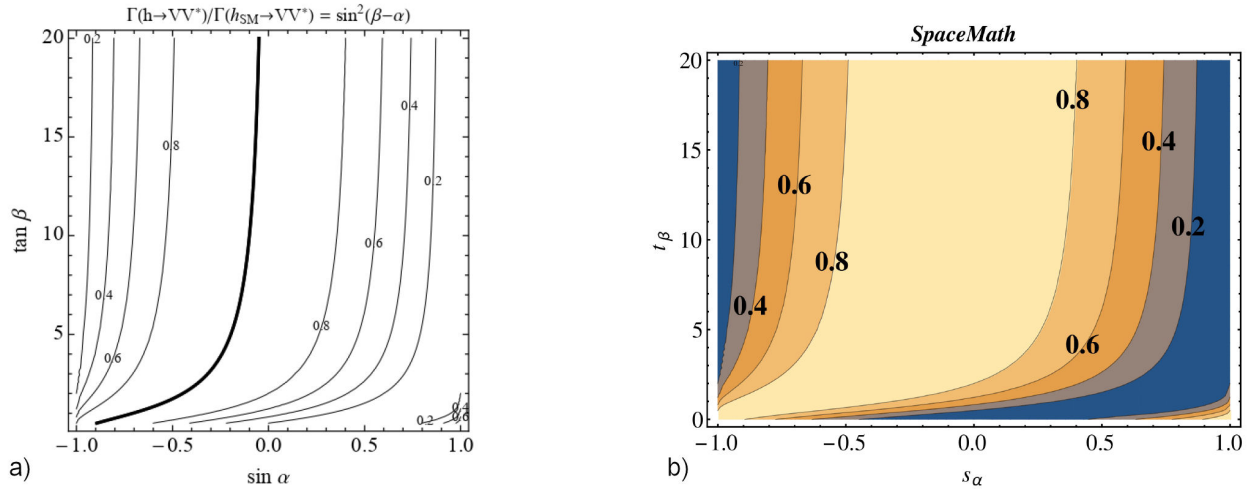

FIGURE 17. Contours of $\Gamma(h \to VV^{\star})/\Gamma(h_{SM}VV^{\star})$ for the SM-like Higgs boson as a function of $\sin\alpha$ and $\tan\beta$ in any of the THDMs. Left: figure taken from [47] and Right: figure generated by `SpaceMath v.2.0`.

TABLE VIII. THMD's hff and hVV couplings.

Coupling	THDM-I	THDM-II	THDM-Lepton Specific	THDM-Flipped
hVV	$\sin(\beta-\alpha)$	$\sin(\beta-\alpha)$	$\sin(\beta-\alpha)$	$\sin(\beta-\alpha)$
hu_iu_i	$\cos\alpha/\sin\beta$	$\cos\alpha/\sin\beta$	$\cos\alpha/\sin\beta$	$\cos\alpha/\sin\beta$
hd_id_i	$\cos\alpha/\sin\beta$	$-\sin\alpha/\cos\beta$	$\cos\alpha/\sin\beta$	$-\sin\alpha/\cos\beta$
$h\ell_i\ell_i$	$\cos\alpha/\sin\beta$	$-\sin\alpha/\cos\beta$	$-\sin\alpha/\cos\beta$	$\cos\alpha/\sin\beta$

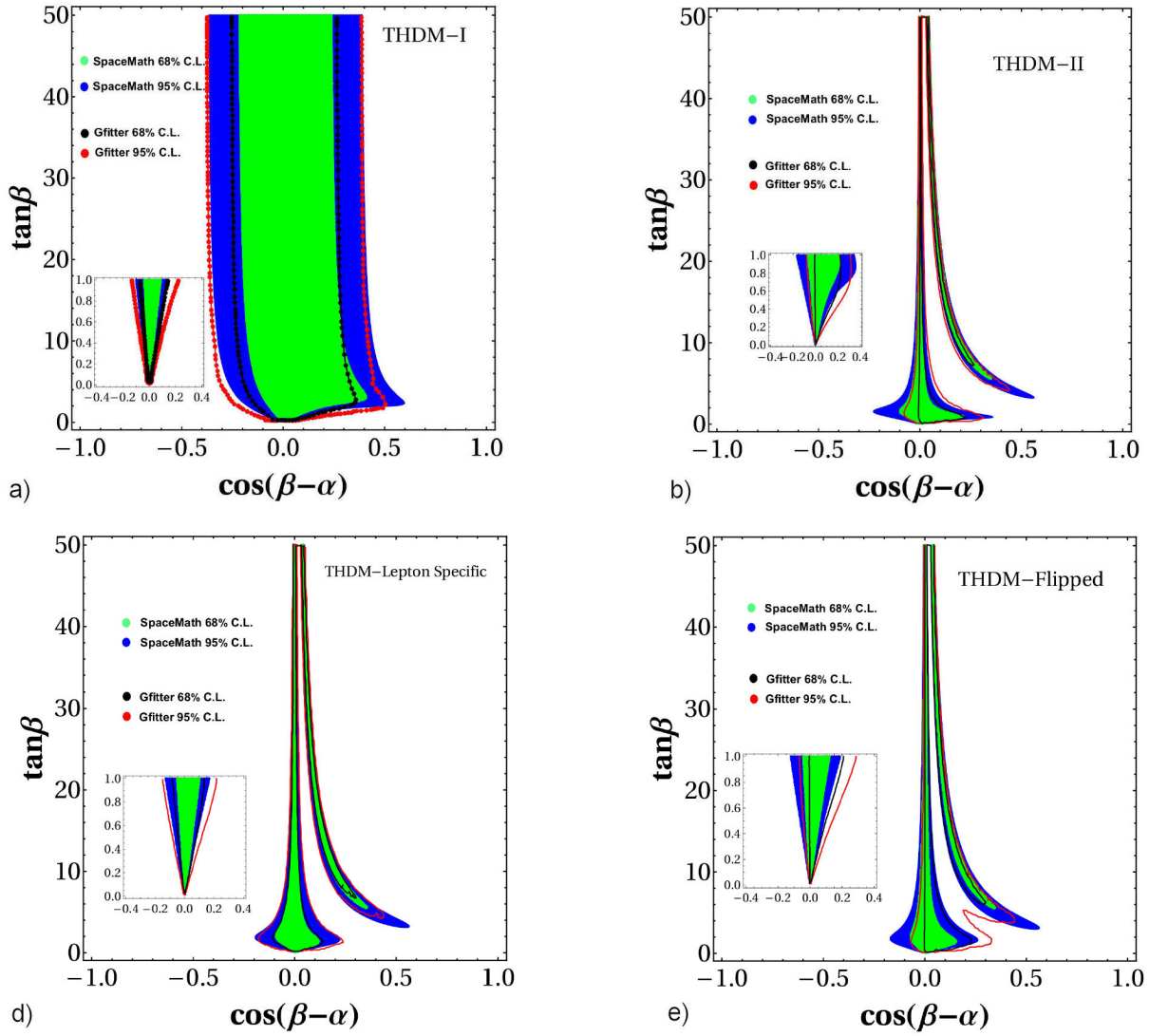

FIGURE 18. Plane $\cos(\beta-\alpha)-\tan\beta$ for different versions of THDM's: a) Type I, b) Type II, c) Lepton Specific, d) Flipped. The plots were generated in `SpaceMath v.2.0`.

```
In[64]:= ContourPlot[kV[ghVV[Tb,Cos[ArcTan[Tb]],
         Sin[ArcTan[Tb]],Sa]^2,{Sa,-1,1},{Tb,0,20}]
```

which generate the graphs displayed in Figs. 15, 16 and 17. The codes that generate these graphs can be found in the `"WorkArea"` directory, whose path is: `SpaceMath/WorkArea/Validation_RX/SPACEMATH_RX-Validation-THDM.nb` or click on the link `"Examples"` once `SpaceMath` was loaded.

In addition, we also show in Fig. 18 the THDM-I, -II, Lepton Specific and Flipped parameter spaces in the $\cos(\beta-\alpha)-\tan\beta$ plane. Again, couplings are shown in Table VIII. We compare our results with the ones reported by authors of Ref. [48]. In these graphs we perform a χ^2 test which is defined as follows:

$$\chi^2=\sum_{i=1}^{n}\left(\frac{O_i-E_i}{\sigma_i}\right)^2, \tag{25}$$

TABLE IX. Comparison of numerical evaluations computed by SpaceMath v1.0 and HDecay. The theoretical framework used is the THDM-I, whose Feynman rules are shown in Table VIII. Results in brackets are those generated via SpaceMath V.2.0.

$\mathcal{BR}(h \to b\bar{b})$	$\mathcal{BR}(h \to \tau\tau)$	$\mathcal{BR}(h \to \mu\mu)$	$\mathcal{BR}(h \to s\bar{s})$	$\mathcal{BR}(h \to c\bar{c})$	$\mathcal{BR}(h \to t\bar{t})$
0.6080 (*0.6080*)	0.6542 (*0.6542*)$\times 10^{-1}$	0.2316 (*0.2316*)$\times 10^{-3}$	0.2294 (*0.2294*)$\times 10^{-3}$	0.2653(*0.2653*)$\times 10^{-1}$	0 (*0*)
$\mathcal{BR}(h \to gg)$	$\mathcal{BR}(h \to \gamma\gamma)$	$\mathcal{BR}(h \to Z\gamma)$	$\mathcal{BR}(h \to WW)$	$\mathcal{BR}(h \to ZZ)$	
0.7041 (*0.7041*)$\times 10^{-1}$	0.2126 (*0.2126*)$\times 10^{-2}$	0.1458 (*0.1458*)$\times 10^{-2}$	0.2005 (*0.2005*)	0.2507 (*0.2507*)$\times 10^{-1}$	
$\mathcal{BR}(h \to AA)$	$\mathcal{BR}(h \to AZ)$	$\mathcal{BR}(h \to W \pm h\mp)$	$\mathcal{BR}(h \to h + h-)$	Γ_h^{tot}	
0 (*0*)	0 (*0*)	0 (*0*)	0 (*0*)	0.4248 (*0.4248*) $\times 10^{-2}$ GeV	

where O_i and E_i are the observed and expected values, respectively, and σ_i indicates uncertainty. The command for plot these figures is:

```
In[65]:= Chi2Rx95[ghtt[-ArcCos[Cba]+ArcTan[tb],tb],
         ghbb[-ArcCos[Cba]+ArcTan[tb],tb],
         ghtautau[-ArcCos[Cba]+ArcTan[tb],tb],
         ghZZ[Sqrt[1-Cba^2]],ghWW[Sqrt[1-Cba^2]],0,
         2000,Cba,tb]

In[66]:= Chi2Rx68[ghtt[-ArcCos[Cba]+ArcTan[tb],tb],
         ghbb[-ArcCos[Cba]+ArcTan[tb],tb],
         ghtautau[-ArcCos[Cba]+ArcTan[tb],tb],
         ghZZ[Sqrt[1-Cba^2]],ghWW[Sqrt[1-Cba^2]],0,
         2000,Cba,tb]
```

Complete instructions can be found at:
$SpaceMath/WorkArea/Validation_RX/SPACEMATH_RX-Validation-THDM-Chi2Rx.nb.

We can observe slight differences between the graphs generated via SpaceMath v.2.0 and those of the Gfitter group, this is due to two sources: 1) The experimental data that SpaceMath considers are the most recent and 2) the Gfitter team includes all production modes of the Higgs boson. Here, it is worth mentioning that even though SpaceMath v.2.0 only has gluon fusion production implemented, our results are highly similar, this may be because it is the dominant channel for the production of the higgs boson.

Finally, we shown in Table IX a comparison between our numerical evaluations and those made via HDecay package [21], which the branching ratios of the Higgs boson decaying to pair of particles ($b\bar{b}$, $s\bar{s}$, $c\bar{c}$, $t\bar{t}$, $\tau^+\tau^-$, $\mu^+\mu^-$, gg, $\gamma\gamma$, $Z\gamma$, W^+W^-, ZZ) in the theoretical framework of the THDM-I are shown. Again, the Feynman rules needed for evaluations are shown in Table VIII, where it can be seen that only two parameters are introduced. We take the same inputs for these free THDM-I parameters as in Ref. [21], namely,

- $\tan\beta = 1.29775$,
- $\alpha = -0.684653$,

and we also consider a Higgs boson mass of $m_h = 125.09$ GeV.

In Table IX, the quantities in brackets are the results generated via SpaceMath. We observe that our results are identical to those HDecay, which is to be expected since we actually reproduced the relevant expressions of the decay widths of the Higgs boson reported in Ref. [49].

5. Conclusions

We have presented a Mathematica package called SpaceMath v.2.0 which generates parameter spaces of Standard Model extensions that are in agreement with current experimental measurements. The physical observables considered in this version are LHC Higgs boson data (and their projections for HL-LHC and HE-LHC) and Lepton Flavor Violating processes. SpaceMath v.2.0 complements the previous version by implementing Machine Learning methods, namely, *Linear Regression*, *Decision Trees*, *Gradiant Boosted Trees*, *Neural Networks and Gaussian Process*, which will help us to predict Benchmark Points to be used directly in numerical evaluations of physical observables associated with particle physics. We show in detail how SpaceMath v.2.0 works by appliying it to the Two-Higgs Doublet Model of type III. The results computed by SpaceMath are in accordance with those reported in the literature by similar packages.

Appendix

A. THDM-III couplings

```
In[67]:= gHmumu[Cab_,tanBeta_,CHImumu_]:=(g/2)*(mmu/mW)*(((Cos[ArcCos[Cab]+ArcTan[tanBeta
         ]]*tanBeta)/Sin[ArcTan[tanBeta]])+((Sqrt[2]*Sqrt[1-Cab^2]*tanBeta)/(g*Sin[ArcTan
         [tanBeta]]))*(mW/vev)*CHImumu)
```

```
In[68]:= gAmumu[tanBeta_,CHImumu_]:=((I*g)/2)*(mmu/mW)*((-tanBeta)+((Sqrt[2]*tanBeta)/(g*
         Sin[ArcTan[tanBeta]]))*(mW/vev)*CHImumu)

In[69]:= ghmumu[Cab_,tanBeta_,CHImumu_]:=(g/2)*(mmu/mW)*((-(Sin[ArcCos[Cab]+ArcTan[
         tanBeta]]*tanBeta)/(Sin[ArcTan[tanBeta]]))+((Sqrt[2]*Cab*tanBeta)/(g*Sin[ArcTan[
         tanBeta]]))*(mW/vev)*CHImumu)

In[70]:= gHtautau[Cab_,tanBeta_,CHItautau_]:=(g/2)*(mtau/mW)*(((Cos[ArcCos[Cab]+ArcTan[
         tanBeta]]*tanBeta)/Sin[ArcTan[tanBeta]])+((Sqrt[2]*Sqrt[1-Cab^2]*tanBeta)/(g*Sin
         [ArcTan[tanBeta]]))*(mW/vev)*CHItautau)

In[71]:= gAtautau[tanBeta_,CHItautau_]:=((I*g)/2)*(mtau/mW)*((-tanBeta)+((Sqrt[2]*tanBeta
         )/(g*Sin[ArcTan[tanBeta]]))*(mW/vev)*CHItautau)

In[72]:= ghtautau[Cab_,tanBeta_,CHItautau_]:=(g/2)*(mtau/mW)*((-(Sin[ArcCos[Cab]+ArcTan[
         tanBeta]]*tanBeta)/(Sin[ArcTan[tanBeta]]))+((Sqrt[2]*Cab*tanBeta)/(g*Sin[ArcTan[

In[73]:= gHee[Cab_,tanBeta_,CHIee_]:=(g/2)*(me/mW)*(((Cos[ArcCos[Cab]+ArcTan[tanBeta]]*
         tanBeta)/Sin[ArcTan[tanBeta]])+((Sqrt[2]*Sqrt[1-Cab^2]*tanBeta)/(g*Sin[ArcTan[
         tanBeta]]))*(mW/vev)*CHIee)

In[74]:= gAee[tanBeta_,CHIee_]:= ((I*g)/2)*(me/mW)*((-tanBeta)+((Sqrt[2]*tanBeta)/(g*Sin[
         ArcTan[tanBeta]]))*(mW/vev)*CHIee)

In[75]:= ghee[Cab_,tanBeta_,CHIee_]:=(g/2)*(me/mW)*((-(Sin[ArcCos[Cab]+ArcTan[tanBeta]]*
         tanBeta)/(Sin[ArcTan[tanBeta]]))+((Sqrt[2]*Cab*tanBeta)/(g*Sin[ArcTan[tanBeta]])
         )*(mW/vev)*CHIee)

In[76]:= gHtt[Cab_,tanBeta_,CHItt_]:=(g/2)*(mt/mW)*(((Sin[ArcCos[Cab]+ArcTan[tanBeta]])/(
         tanBeta*Cos[ArcTan[tanBeta]]))-((Sqrt[2]*Sqrt[1-Cab^2])/(g*tanBeta*Cos[ArcTan[
         tanBeta]]))*(mW/vev)*CHItt)

In[77]:= gAtt[tanBeta_,CHItt_]:=((I*g)/2)*(mt/mW)*((-1/tanBeta)+((Sqrt[2])/(g*tanBeta*Cos
         [ArcTan[tanBeta]]))*(mW/vev)*CHItt)

In[78]:= ghtt[Cab_,tanBeta_,CHItt_]:=(g/2)*(mt/mW)*((Cos[ArcCos[Cab]+ArcTan[tanBeta]]/(
         tanBeta*Cos[ArcTan[tanBeta]]))-((Sqrt[2]*Cab)/(g*tanBeta*Cos[ArcTan[tanBeta]]))
         *(mW/vev)*CHItt)

In[79]:= gHbb[Cab_,tanBeta_,CHIbb_]:=(g/2)*(mb/mW)*(((Cos[ArcCos[Cab]+ArcTan[tanBeta]]*
         tanBeta)/Sin[ArcTan[tanBeta]])+((Sqrt[2]*Sqrt[1-Cab^2]*tanBeta)/(g*Sin[ArcTan[
         tanBeta]]))*(mW/vev)*CHIbb)

In[80]:= gAbb[tanBeta_,CHIbb_]:=((I*g)/2)*(mb/mW)*((-tanBeta)+((Sqrt[2]*tanBeta)/(g*Sin[
         ArcTan[tanBeta]]))*(mW/vev)*CHIbb)

In[81]:= ghbb[Cab_,tanBeta_,CHIbb_]:=(g/2)*(mb/mW)*((-(Sin[ArcCos[Cab]+ArcTan[tanBeta]]*
         tanBeta)/(Sin[ArcTan[tanBeta]]))+((Sqrt[2]*Cab*tanBeta)/(g*Sin[ArcTan[tanBeta]])
         )*(mW/vev)*CHIbb)
```

```
In[82]:= gCHmunmu[tanBeta_,CHImumu_]:= tanBeta-Sqrt[1+tanBeta^2]/Sqrt[2]*mmu*CHImumu

In[83]:= gHmue[Cab_,tanBeta_,CHImue_]:=((Sqrt[1-Cab^2]*tanBeta)/(Sqrt[2]*Sin[ArcTan[
         tanBeta]]))*(Sqrt[mmu*me]/vev)*CHImue

In[84]:= gAmue[tanBeta_,CHImue_]:=((I*Sqrt[mmu*me]*tanBeta)/(Sqrt[2]*vev*Sin[ArcTan[
          tanBeta]]))*CHImue

In[85]:= ghmue[Cab_,tanBeta_,CHImue_]:=((Sqrt[mmu*me]*Cab*tanBeta)/(Sqrt[2]*vev*Sin[
         ArcTan[tanBeta]]))*CHImue

In[86]:= gHtaumu[Cab_,tanBeta_,CHItaumu_]:=((Sqrt[1-Cab^2]*tanBeta)/(Sqrt[2]*Sin[ArcTan[
         tanBeta]]))*(Sqrt[mtau*mmu]/vev)*CHItaumu

In[87]:= gAtaumu[tanBeta_,CHItaumu_]:=((I*Sqrt[mtau*mmu]*tanBeta)/(Sqrt[2]*vev*Sin[ArcTan
         [tanBeta]]))*CHItaumu

In[88]:= ghtaumu[Cab_,tanBeta_,CHItaumu_]:=((Sqrt[mtau*mmu]*Cab*tanBeta)/(Sqrt[2]*vev*Sin
         [ArcTan[tanBeta]]))*CHItaumu

In[89]:= gHtaue[Cab_,tanBeta_,CHItaue_]:=((Sqrt[1-Cab^2]*tanBeta)/(Sqrt[2]*Sin[ArcTan[
         tanBeta]]))*(Sqrt[mtau*me]/vev)*CHItaue

In[90]:= gAtaue[tanBeta_,CHItaue_]:=((I*Sqrt[mtau*me]*tanBeta)/(Sqrt[2]*vev*Sin[ArcTan[
         tanBeta]]))*CHItaue

In[91]:= ghtaue[Cab_, tanBeta_,CHItaue_]:=((Sqrt[mtau*me]*Cab*tanBeta)/(Sqrt[2]
         *vev*Sin[ArcTan[tanBeta]]))* CHItaue

In[92]:= ghWW[Cab_]:=gw*mW*Sqrt[1-Cab^2]

In[93]:= ghZZ[Cab_]:=gz*mZ*Sqrt[1-Cab^2]

In[94]:= gHWW[Cab_]:=gw*mW*Cab

In[95]:= gHZZ[Cab_]:=gz*mZ*Cab

In[96]:= gCH[Cab_,tanBeta_]:=(mW*Sin[ArcTan[tanBeta]-(ArcCos[Cab]+ArcTan[tanBeta])]+mZ
         /(2*CW)*Cos[2 ArcTan[tanBeta]]*Sin[ArcTan[tanBeta]+(ArcCos[Cab]+ArcTan[tanBeta])
         ])*g
```

B. Troubleshooting Common Problems

B.1 Installation

The SpaceMath v.2.0 package includes an automated installation process. However, if this method fails on your system, you can proceed with a manual installation by following the steps outlined below.

```
In[97]:= url = "https://raw.githubusercontent.com/spacemathapp/SpaceMath-v.2.0/alpha/
         BuiltPackage/SpaceMath-2.0.paclet"

In[98]:= out = FileNameJoin[{$UserDocumentsDirectory, "SpaceMath-2.0.paclet"}];
```

```
In[99]:= URLSave[url, out]

In[100]:= PacletInstall[FileNameJoin[{$UserDocumentsDirectory, "SpaceMath-2.0.paclet"}]]

In[101]:= PacletFind["SpaceMath"]
```

B.2 Compatibility with Mathematica

We recommend using `SpaceMath v.2.0` with `Mathematica 13` or later. These releases include the integration of machine learning methods. For users of `Mathematica` 11 or 12, we suggest using `SpaceMath v.1.0` [50].

C. Documentation

When the SpaceMath package is loaded, an interactive menu is displayed (see Fig. **??**). Below, the purpose of each button is described:

- Documentation Center: Provides quick access to SpaceMath documentation, available at `https://spacemaths-organization.gitbook.io/spacemath-documentation`.
- Examples: Access the WorkArea directory, which contains three folders (HiggsBosonData, LFVprocesses and Validation_RX) with notebooks demonstrating the application of the observables to the THDM-III.
- GitHub site: Provides a direct link to the repository hosting the SpaceMath package source code, available at `https://github.com/spacemathapp/SpaceMath-v.2.0`.
- Ask a question: Offers direct access to the forum where users can ask questions to the SpaceMath developers.
- Cite: Provides the necessary information to cite this article.

D. User Guide

The SpaceMath package includes a collection of preloaded examples that users can use as templates for their implementations.

We recommend that users start with the notebooks LHChbd_Rintersection_Expert_Mode.nb, HBD_Kintersection_Expert_Mode.nb, and LFV_intersection_Expert_Mode.nb (located in the Examples directory) as they provide an overview of how to use the SpaceMath package. Specifically, these notebooks utilize the couplings of the THDM-III model. As an example, the structure of the notebook for the `Rintersection` command is divided into the following sections:

1. **Loading the SpaceMath Package**.

Acknowledgments

The work of Marco A. Arroyo-Ureña and T. Valencia-Pérez is supported by "Estancias posdoctorales por México (CONAHCYT)" and "Sistema Nacional de Investigadores" (SNI-CONAHCYT). T.V.P. thanks Dr. Myriam Mondragón for her valuable suggestions during the development of this research work. He also acknowledges support from the UNAM project PAPIIT IN111224 and the CONAHCYT project CBF2023-2024-548.

---

i. $\ell_i \to \ell_j \gamma$ stand for $\tau \to \mu\gamma, \tau \to e\gamma$ and $\mu \to e\gamma$

ii. In general, it can be also induced by other type of particles that change flavor at tree level.

iii. You can execute this command in a notebook of `Mathematica` and will show the location path.

iv. The Yukawa Lagrangian in Eq. (22) only shows the neutral interactions, but the model also predicts two charged scalars, no included there.

v. This command is hidden in other `SpaceMath v.2.0` instructions, generically defined as `Ralgoritm[...]`.

1. N. Arkani-Hamed, A. G. Cohen, E. Katz, and A. E. Nelson. The Littlest Higgs. *JHEP* **07** (2002) 034.
2. Nima Arkani-Hamed, Andrew G. Cohen, and Howard Georgi. Electroweak symmetry breaking from dimensional deconstruction. *Phys. Lett.*, B **513** (2001) 232.
3. Paul H. Frampton and Sheldon L. Glashow. Chiral color: An alternative to the standard model. *Physics Letters B*, **190** (1987) 157.
4. Howard Georgi and Marie Machacek. Doubly charged higgs bosons. *Nuclear Physics B*, **262** (1985) 463 .

5. Haim Harari. A Schematic Model of Quarks and Leptons. *Phys. Lett. B*, **86** (1979) 83.
6. Haim Harari and Nathan Seiberg. The Rishon Model. *Nucl. Phys. B*, **204** (1982) 141.
7. Gordon kane John F. Gunion, Howard E. Haber and Sally Dawson. *The Higgs Hunter's Guide*. Frontiers in Physics, 80. Westview Press, (2000).
8. Hironari Miyazawa. Baryon Number Changing Currents*. *Progress of Theoretical Physics*, **36** (1966) 1266.
9. Rabindra N. Mohapatra and Jogesh C. Pati. Left-Right Gauge Symmetry and an Isoconjugate Model of CP Violation. *Phys. Rev.*, **11** (1975) 566.
10. J. C. Pati and Abdus Salam. Lepton number as the fourth "color". *Phys. Rev. D* **10** (1974) 275.
11. A.M. Polyakov. Quark confinement and topology of gauge theories. *Nuclear Physics B*, **120** (1977) 429.
12. Lisa Randall and Raman Sundrum. A Large mass hierarchy from a small extra dimension. *Phys. Rev. Lett.*, **83** (1999) 3370.
13. Leonard Susskind. Dynamics of spontaneous symmetry breaking in the weinberg-salam theory. *Phys. Rev. D*, **20** (1979) 2619 .
14. S. Weinberg. Implications of dynamical symmetry breaking: An addendum. *Phys. Rev. D*, **19** (1979) 1277).
15. M. A. Arroyo-Ureña, R. Gaitan, R. Martinez and J. H. Montes de Oca Yemha, Dark matter in Inert Doublet Model with one scalar singlet and $U(1)_X$ gauge symmetry, *Eur. Phys. J. C* **80** (2020) 788, https://doi.org/10.1140/epjc/s10052-020-8316-9
16. M. A. Arroyo-Ureña, J. L. Diaz-Cruz, B. O. Larios-López and M. A. P. de León, A private SUSY 4HDM with FCNC in the up-sector, *Chin. Phys. C* **45** (2021) 023118, https://doi.org/10.1088/1674-1137/abcfae
17. Y. Zhang EasyScanHEP collaboration. (Easyscanhep, 2017).
18. F. Bernlochner Sanjay Bloor Torsten Bringmann Andy Buckley Marcin Chrzaszcz Jan Conrad Jonathan M. Cornell Joakim Edsjö Ben Farmer Andrew Fowlie Tomas Gonzalo Julia Harz Sebastian Hoof Paul Jackson Felix Kahlhoefer Anders Kvellestad Nazila Mahmoudi Gregory Martinez James McKay Are Raklev Christopher Rogan Roberto Ruiz de Austri Pat Scott Nicola Serra Roberto Trotta Christoph Weniger Martin White Sebas- tian Wild Peter Athron, Csaba Balázs. (Gambit, 2017).
19. M. Drees, H. Dreiner Florian, D. Jong Soo, K. Frederic, Ponzca Krzysztof Rolbiecki Roberto Ruiz de Austri Liangliang Shang Jamie Tattersall Simon Zeren Wang Thorsten Weber Yuanfang Yue Daniel Dercks, Nishita Desai. (Checkmate, 2014).
20. M. Mühlleitner, M. O. P. Sampaio, R. Santos and J. Wittbrodt, ScannerS: Parameter Scans in Extended Scalar Sectors, [arXiv:2007.02985 [hep-ph]].
21. A. Djouadi, J. Kalinowski, M. Muehlleitner and M. Spira, HDECAY: Twenty$_{++}$ years after, Comput. Phys. Commun. **238** (2019) 214, https://doi.org/10.1016/j.cpc.2018.12.010
22. J. De Blas, D. Chowdhury, M. Ciuchini, A. M. Coutinho, O. Eberhardt, M. Fedele, E. Franco, G. Grilli Di Cortona, V. Miralles and S. Mishima, *et al.* HEPfit: a code for the combination of indirect and direct constraints on high energy physics models, Eur. Phys. J. C **80** (2020) 456, https://doi.org/10.1140/epjc/s10052-020-7904-z
23. H. Flacher, M. Goebel, J. Haller, A. Hocker, K. Monig and J. Stelzer, Revisiting the Global Electroweak Fit of the Standard Model and Beyond with Gfitter, Eur. Phys. J. C **60** (2009) 543-583 [erratum: Eur. Phys. J. C **71** (2011), 1718] https://doi.org/10.1140/epjc/s10052-009-0966-6
24. S. Navas *et al.* [Particle Data Group], Phys. Rev. D **110** 030001 (2024) https://doi.org/10.1103/PhysRevD.110.030001
25. R. Harnik, J. Kopp and J. Zupan, Flavor Violating Higgs Decays, JHEP **03** (2013) 026 https://doi.org/10.1007/JHEP03(2013)026
26. G. Blankenburg, J. Ellis and G. Isidori, Flavour-Changing Decays of a 125 GeV Higgs-like Particle, Phys. Lett. B **712** (2012) 386, https://doi.org/10.1016/j.physletb.2012.05.007
27. M. Beneke, C. Bobeth and R. Szafron, Power-enhanced leading-logarithmic QED corrections to $B_q \to \mu^+\mu^-$, JHEP **10** (2019) 232, [erratum: JHEP **11** (2022) 099] https://doi.org/10.1007/JHEP10(2019)232
28. A. Tumasyan *et al.* [CMS], Measurement of the $B_S^0 \to \mu^+\mu^-$ decay properties and search for the $B^0 \to \mu^+\mu^-$ decay in proton-proton collisions at $\sqrt{s}$ = 13 TeV, Phys. Lett. B **842** (2023) 137955, https://doi.org/10.1016/j.physletb.2023.137955
29. A. J. Buras, J. Girrbach, D. Guadagnoli and G. Isidori, On the Standard Model prediction for BR(Bs,d to mu+ mu-), Eur. Phys. J. C **72** (2012) 2172, https://doi.org/10.1140/epjc/s10052-012-2172-1
30. T. Inami and C. S. Lim, Prog. Theor. Phys. **65** (1981) 297, [erratum: Prog. Theor. Phys. **65** (1981) 1772] https://doi.org/10.1143/PTP.65.297
31. M. Cepeda, S. Gori, P. Ilten, M. Kado, F. Riva, R. Abdul Khalek, A. Aboubrahim, J. Alimena, S. Alioli and A. Alves, *et al.* CERN Yellow Rep. Monogr. **7** (2019) 221, https://doi.org/10.23731/CYRM-2019-007.221
32. G. C. Branco, P. M. Ferreira, L. Lavoura, M. N. Rebelo, M. Sher and J. P. Silva, Theory and phenomenology of two-Higgs-doublet models, Phys. Rept. **516** (2012) 1, https://doi.org/10.1016/j.physrep.2012.02.002
33. F. J. Botella, G. C. Branco and M. N. Rebelo, Minimal Flavour Violation and Multi-Higgs Models, Phys. Lett. B **687** (2010) 194, https://doi.org/10.1016/j.physletb.2010.03.014
34. F. J. Botella, G. C. Branco, M. Nebot and M. N. Rebelo, Flavour Changing Higgs Couplings in a Class of Two Higgs Doublet Models, Eur. Phys. J. C **76** (2016) 161 https://doi.org/10.1140/epjc/s10052-016-3993-0
35. M. A. Arroyo-Ureña, J. L. Diaz-Cruz, E. Díaz and J. A. Orduz-Ducuara, Flavor violating Higgs signals in the Texturized Two-Higgs Doublet Model (THDM-Tx), Chin. Phys. C **40** (2016) 123103, https://doi.org/10.1088/1674-1137/40/12/123103

36. J. Lorenzo Díaz-Cruz, The Higgs profile in the standard model and beyond, Rev. Mex. Fis. **65** (2019) 419, https://doi.org/10.31349/RevMexFis.65.419

37. J. Hernandez-Sanchez, S. Moretti, R. Noriega-Papaqui and A. Rosado, Off-diagonal terms in Yukawa textures of the Type-III 2-Higgs doublet model and light charged Higgs boson phenomenology, JHEP **1307** (2013) 044, https://doi.org/10.1007/JHEP07(2013)044

38. J. E. Barradas Guevara, F. C. Cazarez Bush, A. Cordero Cid, O. Felix Beltran, J. Hernandez Sanchez and R. Noriega Papaqui, Implications of Yukawa Textures in the decay $H^+ \to W^+\gamma$ within the 2HDM-III, J. Phys. G **37** (2010) 115008, https://doi.org/10.1088/0954-3899/37/11/115008

39. A. Cordero-Cid, O. Felix-Beltran, J. Hernandez-Sanchez and R. Noriega-Papaqui, Implications of Yukawa texture in the charged Higgs boson phenomenology within 2HDM-III, PoS CHARGED **2010** (2010) 042, https://doi.org/10.22323/1.114.0042

40. M. Gomez-Bock and R. Noriega-Papaqui, Flavor violating decays of the Higgs bosons in the THDM-III, J. Phys. G **32** (2006) 761, https://doi.org/10.1088/0954-3899/32/6/002

41. M. Arroyo-Ureña and E. Díaz, Dipole moments of charged leptons in the THDM-III with Textures, J. Phys. G **43** (2016) 045002, https://doi.org/10.1088/0954-3899/43/4/045002 [arXiv:1508.05382 [hep-ph]].

42. M. A. Arroyo-Ureña, R. Gaitán-Lozano, E. A. Herrera-Chacón, J. H. Montes de Oca Y. and T. A. Valencia-Pérez, Search for the $t \to ch$ decay at hadron colliders, JHEP **1907** (2019) 041, https://doi.org/10.1007/JHEP07(2019)041

43. M. A. Arroyo-Ureña, T. A. Valencia-Pérez, R. Gaitán, J. H. Montes De Oca and A. Fernández-Téllez, Flavor-changing decay $h \to \tau\mu$ at super hadron colliders, arXiv:2002.04120 [hep-ph].

44. M. Mohammed, M. B. Khan, and E. B. M. Bashier, *Machine Learning: Algorithms and Applications* (1st ed.). (CRC Press 2016). https://doi.org/10.1201/9781315371658

45. I. A. Rauf, *Physics of Data Science and Machine Learning* (1st ed.). (CRC Press 2021).. https://doi.org/10.1201/9781003206743

46. C. A. R. Pinheiro, and M. Patetta, *Introduction to Statistical and Machine Learning Methods for Data Science*. SAS Institute (2021). ISBN: 9781953329622.

47. N. Craig and S. Thomas, Exclusive Signals of an Extended Higgs Sector, JHEP **1211** (2012) 083, https://doi.org/10.1007/JHEP11(2012)083 [arXiv:1207.4835 [hep-ph]].

48. J. Haller, A. Hoecker, R. Kogler, K. Mönig, T. Peiffer and J. Stelzer, Update of the global electroweak fit and constraints on two-Higgs-doublet models, Eur. Phys. J. C **78** (2018) 675, https://doi.org/10.1140/epjc/s10052-018-6131-3

49. A. Djouadi, The Anatomy of electro-weak symmetry breaking. I: The Higgs boson in the standard model, Phys. Rept. **457** (2008) 1, https://doi.org/10.1016/j.physrep.2007.10.004

50. M. A. Arroyo-Ureña, R. Gaitán, and T. A. Valencia-Perez, *SpaceMath version 1.0: A Mathematica package for beyond the standard model parameter space searches*. *Rev. Mex. Fís.* **19** (2022) 020206, https://doi.org/10.31349/RevMexFisE.19.020206